Jour. Geol. Soc. India (2025) 101 (1) : 112–122
https://doi.org/10.17491/jgsi/2025/174065

RESEARCH ARTICLE

Biomarker Evidence of Shifts in Organic Provenance and Depositional Environments of Eocene Carbonaceous Rocks from Petroliferous Barmer Basin, Western Rajasthan, India

Nihar Ranjan Kar[1,2], Devleena Mani[1*], Bala Subrahanyam Seetha[3], E.V.S.S.K. Babu[2], Soumyajit Mukherjee[4**], Swagato Dasgupta[5], and Mohana Krishna Reddy Mudiam[3]

[1]Center for Earth, Ocean and Atmospheric Sciences (CEOAS), University of Hyderabad, Gachibowli, Hyderabad, 500046, India.
[2]Council of Scientific and Industrial Research–National Geophysical Research Institute, Uppal Road, Habsiguda, Hyderabad, 500007, Telangana, India.
[3]Analytical and Structural Chemistry Department, CSIR-Indian Institute of Chemical Technology, Tarnaka, Hyderabad, 500007, India.
[4]Department of Earth Sciences, Indian Institute of Technology Bombay, Powai, Mumbai, 400076, Maharashtra, India.
[5]Department of Applied Geophysics, Indian Institute of Technology (ISM) Dhanbad, Jharkhand, 826004, India.
Email id: *dtiwarisp@uohyd.ac.in (Orcid ID: https://orcid.org/0000-0001-5079-5006), **soumyajitm@gmail.com, smukherjee@iitb.ac.in

Received: 19 July 2024, Revised version accepted 27 August 2024

ABSTRACT

The Barmer Basin of Rajasthan in western India is a proven sedimentary basin with significant oils and natural gas reserves. The basin also possesses lignites and interbedded shales, which are organically-rich and lie close to early mature thermal window. Previous studies have demonstrated that these carbonaceous rocks can be converted into into various hydrocarbon products. We characterise the sedimentary biomarkers and stable carbon isotopes from the Eocene carbonaceous rocks of the Giral lignite mine in the Barmer basin to understand their organic provenance and the depositional environments. Different biomarker ratios of alkanes, hopanes and steranes viz., CPI, OEP, P_{aq}, TAR, TMD, Pr/Ph, LMWH/HMWH, Pr/*n*-C_{17}, Ph/*n*-C_{18}, Ts/Tm and C_{31} 22S/(22S+22R) along with *n*-alkane chromatogram, several bivariate plots, sterane ternary diagram and stable carbon isotope characterize the depositional environment and different types of organic matter (OM) inputs. The Giral lignites deposited in a terrestrial environment fluctuated from oxic to dysoxic with bimodal OM input. The shales were deposited in a marine or lacustrine environment with predominantly aquatic OM input, in contrast to lignites. Shaly lignites show an intermediate depositional environment between lignite and shales and pseudo-bimodal OM input. Sea-level fluctuations led to deposition of various lithotypes under changing depositional environments. Shales and shaly lignites, unlike lignites, exhibit better preservation conditions due to a predominantly anoxic sulphidic environment. The reduced carbon content of shales may be due to a quicker subsidence rate of the basin than peat formation during shale deposition.

Keywords: Rajasthan basin, Giral lignite mine, biomarker, depositional environment, sea-level change.

INTRODUCTION

Sedimentary biomarkers have been used reliably to reconstruct the source vegetation and depositional habitats of peatlands (Bechtel et al., 2004; Kar et al., 2022). High-resolution biomarker data from organic-rich rocks such as lignites and (carbonaceous) shales can connote palaeoenvironments and climate, oxidation-reduction conditions, levels of microbial alteration and palaeo-vegetation (Stefanova et al., 2002; Kumar et al., 2022).

OM comprises carbon-containing materials originating from (once) living organisms. Several environmental elements (e.g., temperature, pressure, presence of microbes, oxygen level) are connected to the preservation of OM (Henrichs, 1993). Biomarkers connote the genesis of organic materials and the conditions under which they formed. By examining the abundance, limitations and ratios of these markers in sediments, one can characterise geologic Eras and their depositional environments (Peters et al., 2005a). While the compositional ratios of the sedimentary biomarkers provide information about the depositional environment, type of OM input and maturity, the stable isotope ratio of carbon, and nitrogen in the organic fraction are employed to distinguish marine and terrestrial sources, paleoenvironments and the secular variations associated with the global biogeochemical processes (Mani et al., 2022).

The abundance of organic productivity, nutrient concentrations and upwelling, reducing environment, restricted water circulation, absence of bioturbation, fine-grained sediment particles mostly < 2 μm and optimal sedimentation rates contribute to OM content and quality in sediments and rocks (Bjorlykke, 2015; Mani et al., 2022). The degradation and preservation of OM vary depending on the specific environment. For example, preservation potential and quality for oil-prone OM is better in a marine anoxic depositional environment than terrestrial oxic environment (Peters et al., 2005a). Thus, the depositional environment strongly controls the characteristics of source rocks and in conjunction with OM type, governs the oil and gas generation attributes of a source rock.

This study analyzes sedimentary biomarkers and stable organic carbon isotopes to interpret the depositional environment and hydrocarbon potential of Eocene source rocks in the Barmer Basin, Rajasthan. The Rajasthan basin, comprised of few sub-basins, is classified as a Category-I sedimentary basin of India with significant ongoing hydrocarbon production. India's largest on-land oil field Mangala is located in this basin (DGH, 2018). The basin is remarkable for its massive lignite mines, consisting of thick organic-rich layers of lignites, shales and shaly lignites, in addition to its prodigious oil resources (Kar et al., 2022). Several researchers have examined the palynologic, petrographic and physicochemical characteristics of Rajasthan lignites for more than a hundred years (Oldham, 1886, Dolson et al., 2015; Singh et al., 2016; Kar et al., 2022). A detail of the organic geochemical work carried out for western India, comprising both Rajasthan and Gujarat is given in the Repository Table 1. The Eocene lignites from the Giral mine in Barmer Basin exhibit encouraging results regarding their source rock potential and the possibility of viable conversion into unconventional energy resources (Kar et al., 2022).

Although several studies have indicated a marine incursion in the Barmer basin (Sharma 2007; Singh et al., 2016, 2019), no work particularly correlates and distinguishes the various lithotypes and their OM properties, which can constrain reliably the depositional environments. In this article, depositional environments for distinct lithotypes- shales, lignites and shaly lignites from Eocene Formations of the Giral mine- have been distinguished using biomarkers and stable carbon isotope study.

GEOLOGY AND STRATIGRAPHY

The Rajasthan basin (Fig. 1a), which covers ~ 1,26,000 km^2, has proven economic hydrocarbon production (DGH, 2018). Figure 1a presents the important lignite mines of Rajasthan. The Giral mine (Fig. 1b) lies ~ 43 km north of the Barmer city. The mine is part of the Dharvi Dundar Formation (DDF) within the Jagmal Group (Dolson et al., 2015; Farrimond et al., 2015; Kar et al., 2022). The DDF, deposited during the Early Eocene Epoch mostly in a lacustrine environment, consists of alternating lignite, sandstone, and shale deposits (Dolson et al., 2015; Farrimond et al., 2015; Kar et al., 2022). The Giral Member functions as a source, reservoir, and seal (Farrimond et al., 2015). This unit is a continuation of the fossil-rich Akli Formation from the Late Paleocene (Thanetian) through the Early Eocene (Farrimond et al.,

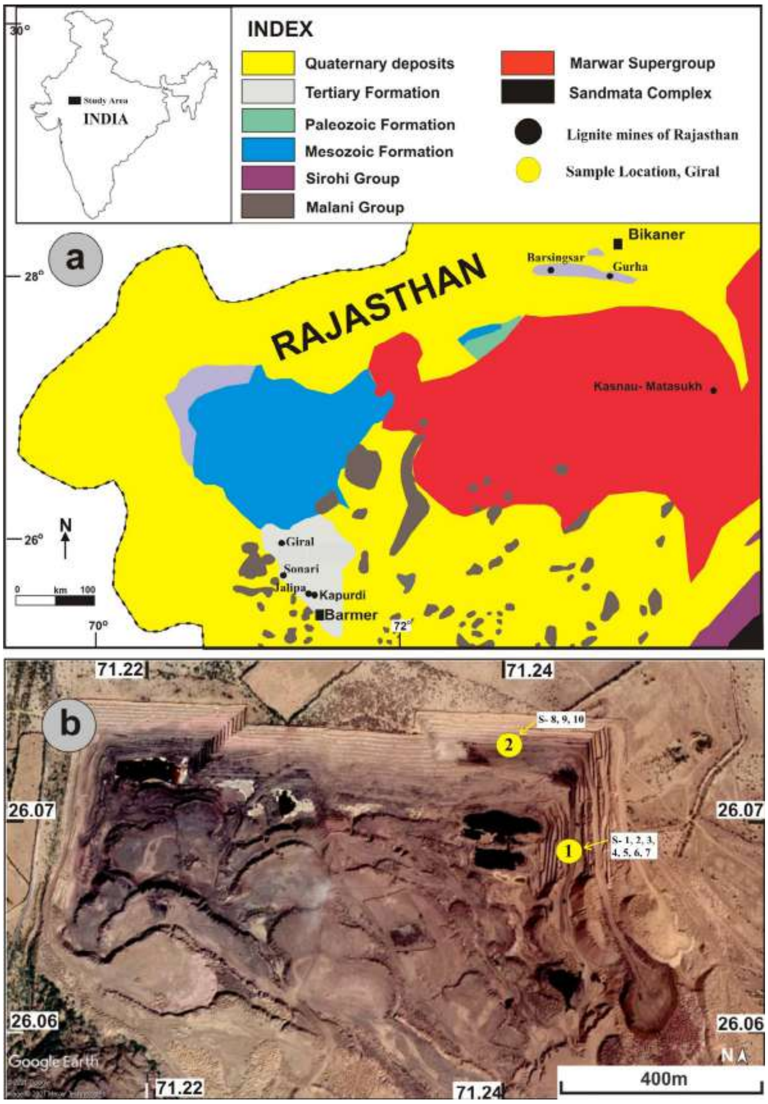

Fig 1a. Geological map of Barmer basin (modified after Roy and Jakhar, 2002). Locations of samples Giral and Sarnoo are plotted. Important lignite mines in Rajasthan are plotted. b. Google Earth image of the Giral mine. Yellow circles: Sample locations. Location 1 marks the location for samples 1 to 7 (details in Fig. 2) and location 2 represents the sample location for samples 8 to 10 (details in Fig. 3), Reproduced from figures 1a,b of Kar et al. (2022).

2015; Kar et al., 2022). The Giral Member was primarily deposited in a lacustrine environment (Raju and Mathur, 2013, Dolson et al., 2015; Kar et al., 2022). Prasad et al. (2020) identified five units of the rock sequence in the Giral mine using dinoflagellate studies and related them to system tracts and incursions as described by Singh et al. (2015). The primary source of OM input was mangroves (Raju and Mathur, 2013). Ostracods, dinoflagellates and fish have also been documented , which suggests that the basin experienced marine influence either from the south (Dolson et al., 2015; Farrimond et al., 2015) or from the Devikot high area from the north.

MATERIALS AND METHODS

Introductory information, solvent extraction, column chromatography, Gas Chromatography Mass Spectrometry (GC-MS) analysis, kerogen separation and carbon isotope analysis were done as per standard processes (Repository material) performed on the ten samples of lignites, shaly lignites from the Giral mine (Figs. 1b, 2 & 3).

RESULTS

All the samples contain saturated hydrocarbons in the nC_{12} - nC_{35} range, acyclic isoprenoids, hopanes and steranes. The distribution of *n*-alkane is bimodal with peak maxima at nC_{14} and nC_{27} for lignites, pseudo bimodal with peak maxima at nC_{14} and nC_{29} for shaly lignites and unimodal with a peak maximum at nC_{14} for shales (Fig. 4). Hopane (*m/z* 191) isomers are abundant consistently in the range of nC_{27} to nC_{33}, with C_{29} 17αH, 21βH-norhopane being the most abundant for lignites and C_{28} tricyclic terpane (22R) for shaly lignites and shales (Fig. 5; Table 1). The steranes (*m/z* 217) isomers have a consistent abundance in the range nC_{27} to nC_{30}, with C_{28} ααα sterane (20S) being the most abundant in lignites and C_{27} αβ diasterane (20S) in shaly lignites and shales (Fig. 6; Table 2).

The carbon preference index (CPI) of lignites, shaly lignite and shales range from 0.77-0.9 (averaging ~ 0.84), 0.67-0.81 (~ 0.74) and 0.68-0.74 (~ 0.7), respectively (Table 3). The CPI-1 and CPI-2 values show a relatively higher range for lignites (~ 3.87 and ~ 0.16) followed by shaly lignites (~ 2.92 and ~ 0.07) and shales (~ 2.11 and ~ 0.07) (Table 3). The odd-to-even preference (OEP), OEP-1 and OEP-2 values show comparably higher values for lignites (~ 0.99 and ~ 1.54), followed by shaly lignites (~ 0.53 and ~ 0.16) and shales (~ 0.44 and 0.81) (Table 3). The proxy ratio (P_{aq}) shows a higher range for shales (0.37-0.45, ~ 0.41) followed by shaly lignites (0.26-0.38, ~ 0.3) and lignites (0.16-0.25, ~ 0.21). The terrestrial aquatic ratio (TAR) shows a significantly higher range for lignites (9.96-17, ~ 12.9) followed by shaly lignites (3.36-9.33, ~ 6.09) and shales (1.82-5.33, ~ 3.04). Similarly, the terrestrial marine discriminants (TMD) show a relatively higher range for lignites (5.93-8.61, ~ 6.96). This is followed by shaly lignites (3.07-7.16, ~ 4.93) and shales (1.88-4.85, ~ 2.93) (Table 3). The pristane upon phytane (Pr/Ph) ratio of the examined samples shows a predominantly higher ratio for lignites (3.56-10.73, ~ 6.81). This is followed by shaly lignites (0.76-1.19,

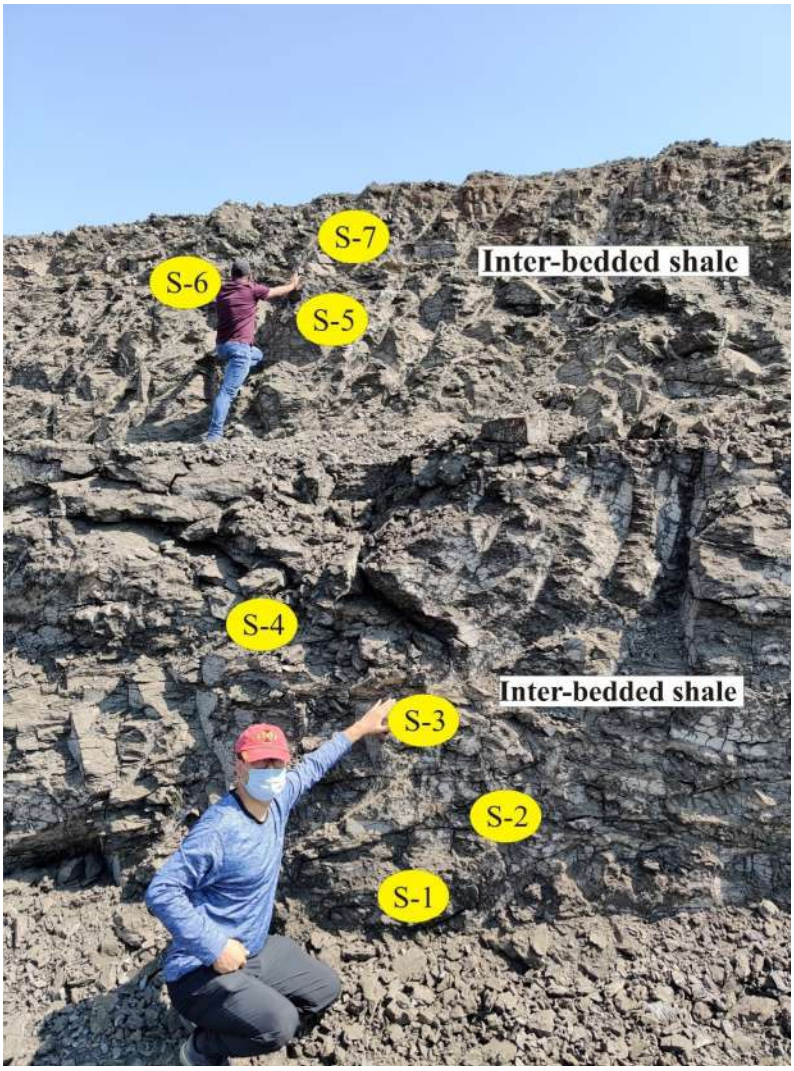

Fig 2. Outcrop in Giral mine showing sample locations (S-1 to S-7). Two thinly interbedded shale horizons were found between lignite deposits. 26.04334 N, 071.14923 E. Reproduced from figure 2 of Kar et al. (2022).

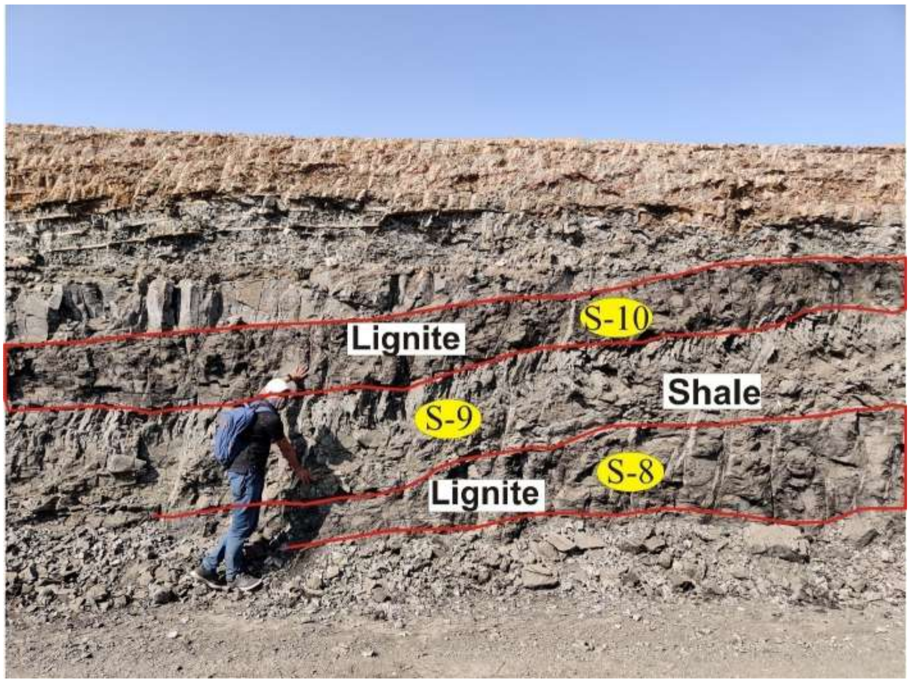

Fig 3. Sample locations from the Giral mine (S-8 to S-10). Two coal seams with an interbedded shale horizon. 26.04334 N, 071.14923 E. Reproduced from figure 3 of Kar et al. (2022).

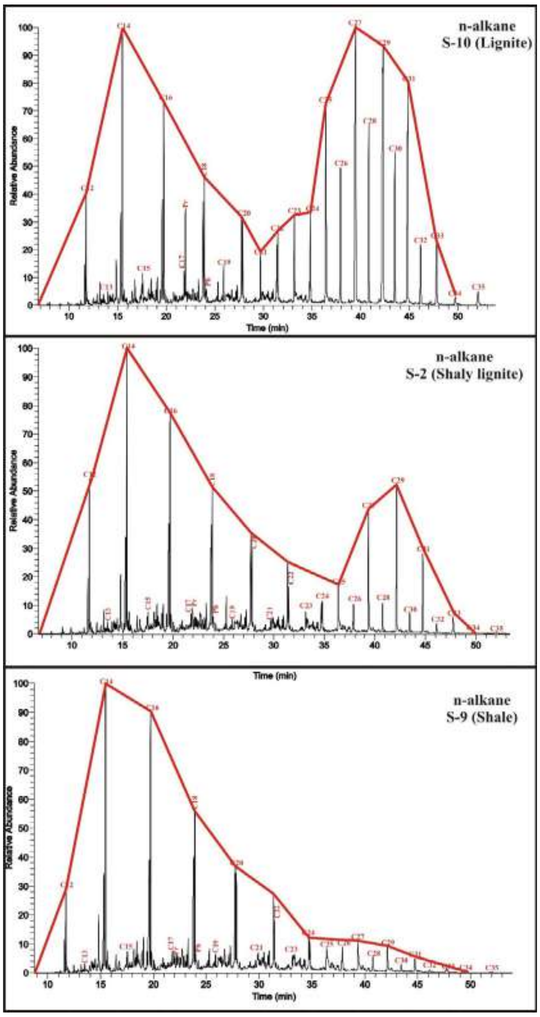

Fig 4. Ion extracted *n*-alkane (*m/z* 57, 71, 85) chromatogram showing a clear biomodal distribution for lignite (S-10), pseudo-bimodal distribution for shaly lignite (S-2) and unimodal distribution for shale (S-9).

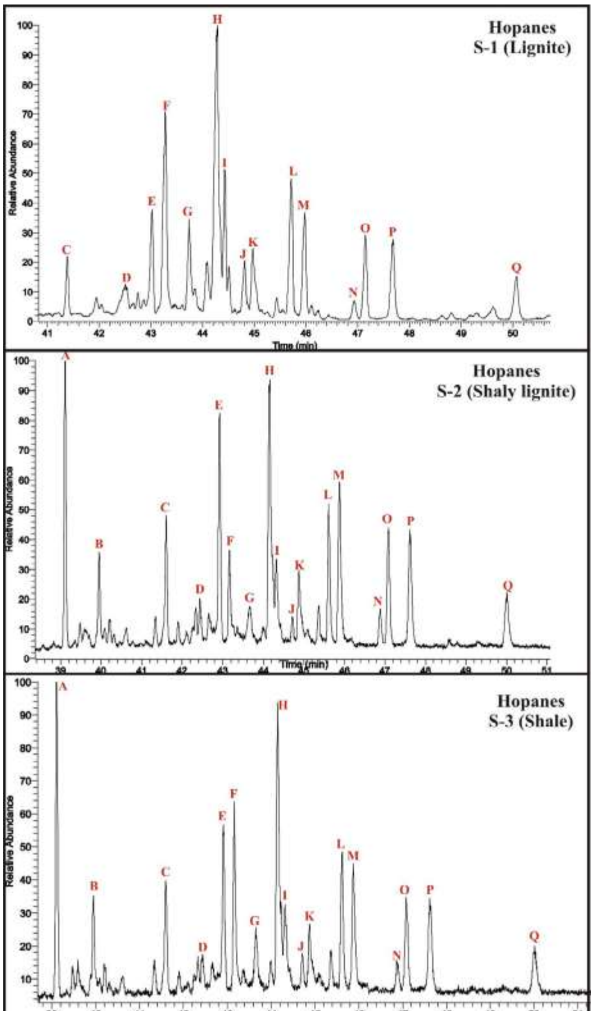

Fig 5. Ion extracted hopane (*m/z* 191) chromatogram of lignite (S-1), shaly lignite (S-2) and shale (S-3). The identified hopanes are listed in Table 1.

Table 1. List of hopanes (*m/z* 191 filtered) found in examined lignites, shaly lignites and shales.

A	C_{28} Tricyclic terpane (22R)
B	C_{29} Tricyclic terpane (22R)
C	C_{27} 18αH- trisnorhopane (Ts)
D	C_{27} 17αH- trisnorhopane (Tm)
E	C_{28} 17αH, 18αH, 21βH-28, 30-bisnorhopane
F	C_{31} Tricyclic terpane (22R)
G	C_{29} 17αH, 21βH 25-norhopane
H	C_{29} 17αH, 21βH-norhopane
I	C_{29} 18αH-norneohopane (29Ts)
J	C_{30} 17αH diahopane
K	C_{29} 17βH,21αH-normoretane
L	C_{30} 17αH, 21βH-hopane
M	C_{30} 30-Nor-29-homo-17αH-hopane
N	C_{31} 17αH, 21βH-homohopane (22S)
O	C_{31} 17αH, 21βH-homohopane (22R)
P	C_{30} gammacerane
Q	C_{33} 17αH, 21βH-trishomohopane (22S)

Table 2. List of Steranes (*m/z* 217 filtered) found in examined lignites, shaly lignites and shales.

A	C_{27} αβ diasterane (20S)
B	C_{28} αβ diasterane (20R)
C	C_{27} ααα sterane (20R)
D	C_{27} αβ diasterane (20S)
E	C_{28} ααα sterane (20S)
F	C_{29} αβ diasterane (20R)
G	C_{28} αββ sterane (20R)
H	C_{28} ααα sterane (20R)
I	C_{29} ααα sterane (20S)
J	C_{29} αββ sterane (20R)
K	C_{29} αββ sterane (20S)
L	C_{29} ααα sterane (20R)
M	C_{30} ααα sterane (20S)

~ 0.91) and shales (0.61-0.85, ~ 0.76). Similarly, the Pr/nC_{17} shows a relatively higher range for lignites (2.88-5.13, ~ 4.46) followed by shaly lignites (1.08-1.4, ~ 1.2) and shales (0.72-1.11, ~ 0.9) (Table 3). The low molecular weight hydrocarbons (LMWH) to high molecular weight hydrocarbons (HMWH) show a higher value for shales (1.84-2.93, ~ 2.59) followed by shaly lignites (0.94-2.44, ~ 1.7) and lignites (0.23-0.84, ~ 0.58) (Table 3).

The maturity indicator parameter Ts/Tm ratio varies between 0.49-0.56 (~ 0.53) for lignites, 0.75-0.79 (~ 0.77) for shaly lignites and 0.73-0.81 (~ 0.78) for shales (Table 4). The C_{31} 22S/(22S+22R) ratio of lignites varies between 0.06 to 0.17 (~ 0.10), 0.12-0.14 (~ 0.13) for shaly lignites and 0.09-0.13 for shales (~ 0.11) (Table 4). The sterane abundances (in %) for lignites peak at C_{28} and C_{29}, whereas the peak for shaly lignites and shales is at C_{27} (Table 4).

The $\delta^{13}C$ value of shaly lignites varies from -23.3 to -25.0 ‰ (~ 24.33 ‰) and shale ranges from -24.5 to -25.0 ‰ (~ 24.84 ‰), while lignites range from -22.3 to -25.8 ‰ (~ 23.58 ‰) (Table 4).

DISCUSSIONS

n-alkanes and isoprenoids

The distribution of *n*-alkane and acyclic isoprenoids in the studied rock samples demonstrate a distinct identity in the source of OM and depositional environment between the examined Eocene lignites, shaly lignites and shales (Fig. 4). The dominance of short-chain *n*-alkanes, such as nC_{15}, nC_{17} and nC_{19}, indicates a microbial source with a marine to lacustrine depositional environment (Gelpi et al., 1970; Peters et al., 2005b), whereas the predominance of long-chain *n*-alkanes, e.g., nC_{27}, nC_{29} and nC_{31} are characterized by a higher plant input with a terrigenous environment of deposition (Eglinton and Hamilton, 1967; Peters et al., 2005b). Lignites with a bimodal peak maxima at nC_{14} and nC_{27} demonstrates an OM input from both higher plant and algae sources with a diversified depositional environment. Similarly, the pseudo bimodal *n*-alkane distribution for shaly lignites with apeak maxima at nC_{14} and nC_{29} indicates an OM input from both higher plant and microbial sources, but predominately from microbial sources, with an assorted depositional environment. A dominant microbial source of OM input with a marine/aquatic environment of deposition is indicated by the unimodal *n*-alkane distribution for shales with peak maxima at nC_{14} (Fig. 4).

CPI1 values for OM generated from vascular plants range from 5 to 10 (Commendatore et al., 2012; El Nemr et al., 2016). Aquatic submergent plants and emergent vegetation contribute to a decrease in the CPI1 value below 5. For the examined samples, lignite has the highest CPI1 value, followed by shaly lignite and shales. The sequence indicates a stronger aquatic influence for shales than lignites. However, an overall CPI1 score of < 5 denotes the OM input from aquatic submergent vegetation species (Table 3). Additionally, the sources of short-chain *n*-alkanes may be determined using the CPI2 parameter (Punyu et al., 2013; Kumar et al., 2022). Petroleum sources may be indicated by CPI2 values of 1 or close to 1, whereas values < 1 are linked to microbial activity (Clark and Blumer, 1967; Kumar et al., 2022). The CPI2 values are greatest for lignites, followed by shale lignite and shales, indicating that shales have higher levels of microbial activity than lignites.

An OEP value < 1 denotes an even-over-odd preference with OM input primarily coming from aquatic vegetation, whereas, a value of OEP > 1 denotes an odd-over-even preference with OM input predominantly coming from terrestrial vegetation (Scalan and Smith, 1970; Kumar et al., 2022). An OEP1 value <1 for all samples (except the S-10 lignite) under investigation denotes an even-to-odd preponderance (EOP) of *n*-alkanes. The highest value is found in lignites, followed by shaly lignites and shales (Table 3). The sequence suggests an abundance of aquatic OM input to the study area. In contrast to medium-chain homologs from aquatic plants, long-chain *n*-alkanes from waxy terrestrial plants show a stronger preference for odd carbons (Tewari et al., 2017, Kumar et al., 2022). Thus, the likelihood that OM originated from waxy plants increases with elevated OEP2 concentrations. However, biodegradation of the low-carbon *n*-alkanes and/or OM generated from aquatic plants may decrease the OEP2 levels (Kumar et al., 2022). The examined samples show the highest OEP2 value for lignites, followed by shales and shaly lignites. An OEP2 value >1 for lignites and <1 for both shale and shaly lignites indicate paleovegetation changes and accompanying alterations in the *n*-alkane signature of the supplied OM.

The P_{aq} results indicate the type of macrophytes derived from the terrestrial OM. P_{aq} values below 0.1 suggest terrestrial plant input, values between 0.1 and 0.4 indicate emergent macrophytes and values ranging from 0.4 to 1 indicate submerged or floating macrophytes (Ficken et al., 2000; Kar et al., 2024). A P_{aq} value of 0.41 for shales

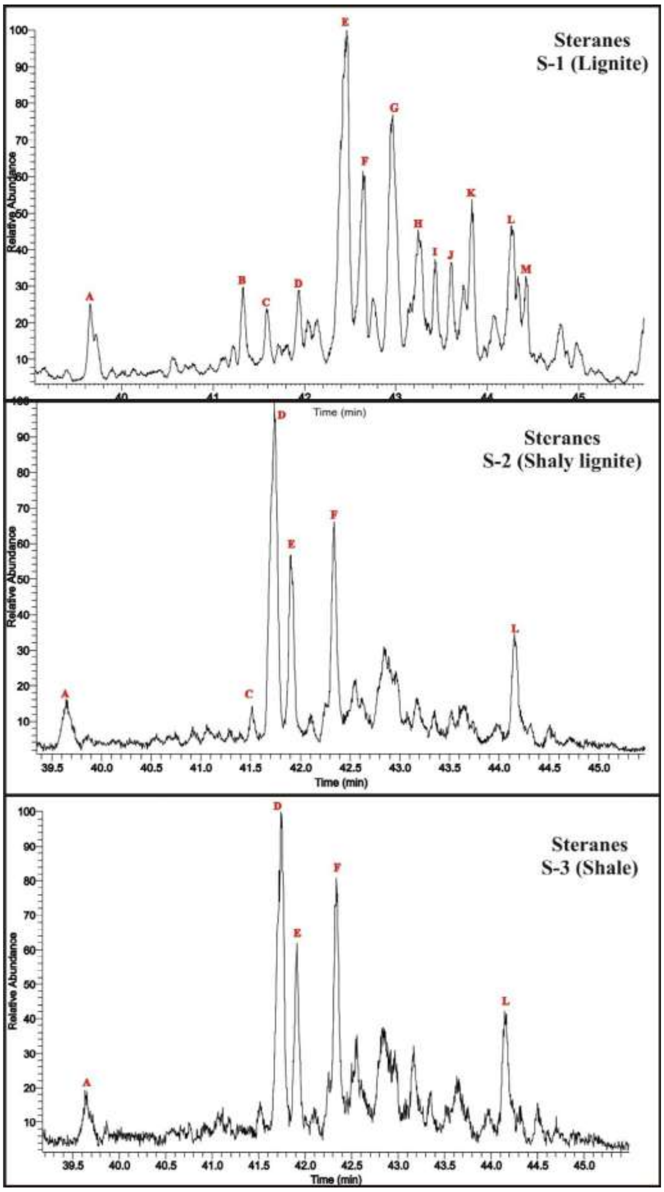

Fig 6. Ion extracted steranes (*m/z* 217) chromatogram of lignite (S-1), shaly lignite (S-2) and shales (S-3) of Giral lignite mine, Barmer basin. The identified steranes are listed in Table 2.

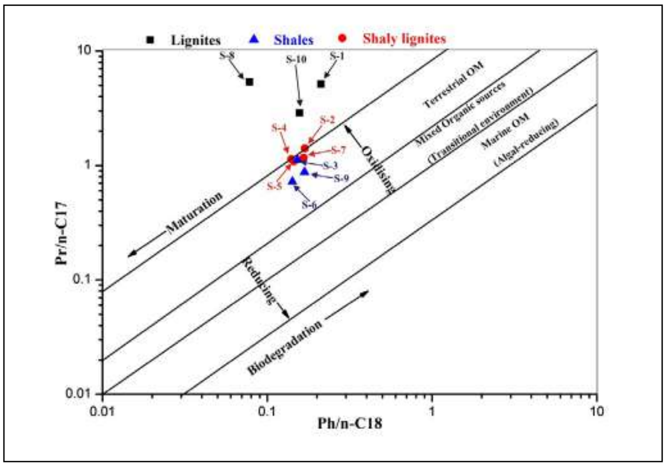

Fig 7. Cross-plot between Pr/n-C_{17} & Ph/n-C_{18} showing the type of OM input and depositional condition.

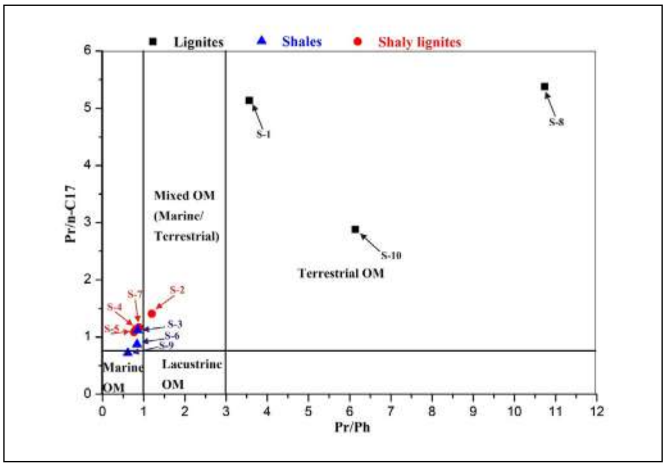

Fig 8. Cross-plot between Pr/n-C_{17} & Pr/Ph showing the type of OM input for lignites (S- 1, 8, 10), shales (S- 3, 6, 9) and shaly lignites (S-2, 4, 5, 7) from Giral mine.

Table 3. Important Biomarker n-alkane ratios were found in examined lignites, shaly lignites and shales. (Calculation detail presented in the Repository file).

SAMPLE ID	LITHOLOGY	CPI	CPI 1	CPI 2	OEP1	OEP2	P_{aq}	TAR	TMD	Pr/Ph	Pr/n-C_{17}	Ph/n-C_{18}	LMWH/ HMWH
GM-1	Lignite	0.77	4.84	0.11	0.67	1.96	0.16	9.96	5.93	3.56	5.14	0.21	0.84
GM-8	Lignite	0.86	4	0.14	0.92	1.63	0.21	11.6	6.34	10.7	5.38	0.08	0.68
GM-10	Lignite	0.9	2.76	0.22	1.4	1.02	0.25	17	8.61	6.14	2.88	0.16	0.24
GM-2	Shaly lignite	0.81	4.11	0.09	0.76	1.64	0.26	9.33	7.16	1.2	1.41	0.17	0.95
GM-4	Shaly lignite	0.73	2.92	0.06	0.38	1.18	0.26	5.32	4.65	0.81	1.14	0.14	2.07
GM-5	Shaly lignite	0.67	2.11	0.07	0.4	0.89	0.38	3.36	3.07	0.76	1.09	0.15	2.44
GM-7	Shaly lignite	0.75	2.53	0.08	0.56	0.94	0.29	6.35	4.82	0.88	1.17	0.17	1.38
GM-3	Shale	0.74	2.99	0.06	0.57	1.19	0.37	5.33	4.85	0.85	1.12	0.15	1.84
GM-6	Shale	0.68	1.71	0.08	0.34	0.63	0.41	1.98	2.06	0.61	0.72	0.14	3.01
GM-9	Shale	0.69	1.63	0.08	0.42	0.6	0.45	1.82	1.88	0.84	0.88	0.17	2.94

Table 4. Hopanes, sterane and carbon isotope data for lignites, shaly lignites and shales.

SAMPLE ID	LITHOLOGY	Ts/(Ts+Tm)	C_{31} 22S/(22S+22R)	%C_{27}	%C_{28}	%C_{29}	$\delta^{13}C$ (‰)
GM-1	Lignite	0.54	0.064301092	11.49724	50.77913	37.72363	-25.807
GM-8	Lignite	0.57	0.068947263	11.95668	48.01503	40.02829	-22.595
GM-10	Lignite	0.5	0.17837552	13.32429	47.39385	39.28186	-22.35
GM-2	Shaly lignite	0.74	0.147429643	52.06219	17.06229	30.87552	-23.314
GM-4	Shaly lignite	0.78	0.135107322	52.92743	16.73019	30.34238	-24.208
GM-5	Shaly lignite	0.82	0.125352031	61.19262	13.40228	25.4051	-24.795
GM-7	Shaly lignite	0.79	0.125380129	56.87375	16.42285	26.7034	-25.009
GM-3	Shale	0.79	0.118470223	45.03519	15.92266	39.04215	-25.005
GM-6	Shale	0.77	0.131579807	42.76282	16.09441	41.14277	-24.971
GM-9	Shale	0.76	0.098887114	43.57223	17.30948	39.11829	-24.553

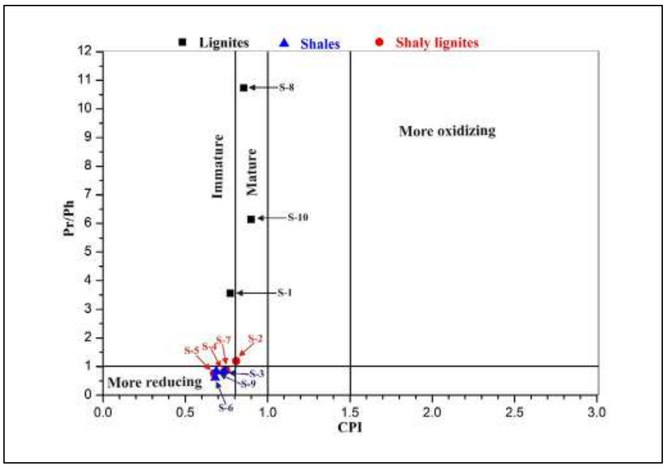

Fig 9. Cross-plot between Pr/Ph and CPI showing the maturity and depositional condition for lignites (S- 1, 8, 10), shales (S- 3, 6, 9) and shaly lignites (S- 2, 4, 5, 7) from Giral mine.

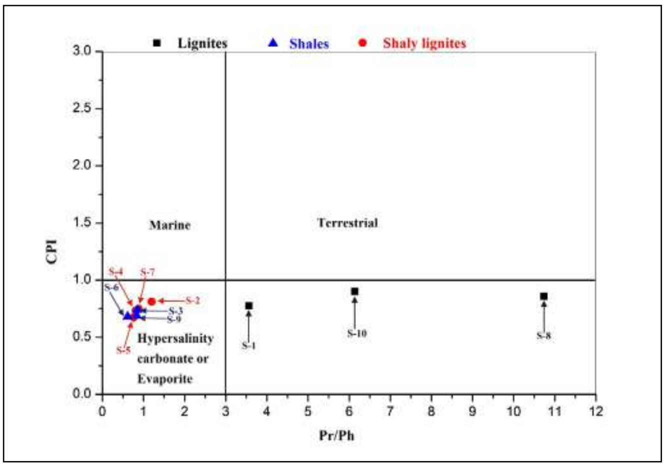

Fig 11. Cross-plot between CPI and Pr/Ph showing the depositional environment for lignites (S- 1, 8, 10), shales (S- 3, 6, 9) and shaly lignites (S- 2, 4, 5, 7) from Giral mine.

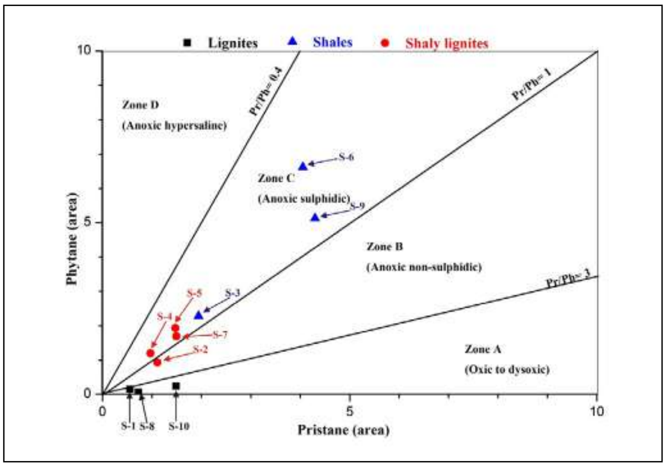

Fig 10. Cross-plot between Pristane and Phytane showing the environment of deposition for lignites (S- 1, 8, 10), shales (S- 3, 6, 9) and shaly lignites (S- 2, 4, 5, 7) from Giral mine.

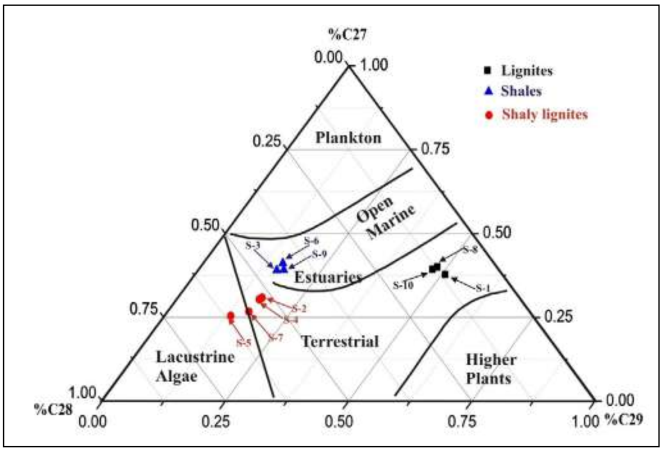

Fig 12. Sterane triangular plot (Huang and Meinschein, 1979; Peters et al., 2005b) marking the source of OM input for different lithology.

indicates submerged/floating macrophytes. A magnitude of 0.21 for lignites shows emerging macrophytes (Table 3).

A greater TAR value denotes a terrigenous input that predominates, whereas a lower magnitude denotes an aquatic input (Bourbonniere and Meyers, 1996; Peters et al., 2005b). For the studied samples, lignites are distinguished by having the highest TAR value, followed by shaly lignites and shales. This shows a shift in OM input while different lithotypes deposited (Table 3). In line with TAR, a lower TMD value reflects an aquatic input and a higher magnitude connotes a dominating terrestrial OM input (Chairi, 2018). The greatest TMD value was observed for lignites, followed by shaly lignites and shales, indicating a transition of OM input to the location (Table 3).

Similarly, LMWH/HMWH < 1 indicates input from higher terrestrial plants, sedimentary microorganisms, and marine animals, while a ratio > 1 suggests an aquatic input (Gearing et al., 1976; Kar et al., 2024). Shales and shaly lignites exhibit a ratio > 1, indicating aquatic input, except lignites, which show a ratio < 1 (Table 3). This ratio is consistent with previous biomarker ratios, which suggest a transition in OM input from terrestrial to marine sources during the formation of different lithotypes.

The Pr/Ph ratio is commonly utilised as markers for different depositional environments (Didyk et al., 1978; Peters et al., 2005b). A ratio > 3 indicates oxidised terrestrial plant OM (Powell, 1984). Pr/Ph ratio < 2 indicates aquatic deposition in fresh, brackish, or marine waters (reducing conditions). Ratios between 2-4 suggest fluvio-marine and coastal swamp environments, while up to 10 suggest peat swamp deposition with significant OM oxidation (Lijmbach, 1975). A Pr/Ph ratio of 6.81 for lignites indicates an oxic depositional habitat similar to a peat swamp, but a ratio of < 1 for shaly coal (~ 0.91) and shale (~ 0.76) indicates an aquatic reducing environment (Table 3).

Using the *n*-alkane data, several bivariate plots were created (Figs. 7-11) to characterize the depositional environment and the source of OM input. For the deposition of lignites from shaly lignite and shales, all other graphs (Figs. 8-11), except Pr/n-C_{17} & Ph/n-C_{18} (Fig. 7), clearly identify a distinct source as well as the depositional environment. Plots of Pr/n-C_{17} vs. Pr/Ph (Fig. 8) characterise a terrestrial source for lignites, a mixed source for shaly lignites, and a source mostly marine for shale. The depositional environment was verified for each lithotype using three bivariate plots (Figs. 9-11). As per the CPI vs. Pr/Ph diagram, lignites have an oxidising field, while shales and shaly lignites have a stronger reducing field (Fig. 9). The pristane vs. phytane diagram differentiates lignites, indicating oxic to dysoxic conditions, from shaly lignites and shales, which represent anoxic sulphidic conditions (Fig. 10). The CPI vs. Pr/Ph graphic similarly depicts a terrestrial environment for lignites and a carbonate-to-evaporite deposit in a hypersaline environment for shaly lignites and shales (Fig. 11). These graphs (Figs. 9-11) show how the depositional environments of lignites, shaly lignites and shales differ. The maturity diagram (Fig. 9) indicates that the analysed samples are primarily immature.

Triterpanes (*m/z* 191)

Hopanes are pentacyclic triterpanes that develop from bacterial membrane precursors (Ourisson et al., 1979; Peters et al., 2005b). Among all hopanes, Ts/(Ts+Tm) ratio is frequently used to access the thermal maturity and the depositional environment of OM (Peters et al., 2005b; Mani and Kar, 2024). As the percentage of shale in calcareous facies rises, the ratio of Ts (trisnorneohopane) to Tm (trisnorhopane), usually > 0.5, rises as well (Hunt, 1995; Roushdy et al., 2010). The ratio is high for environments near shales and low for environments near carbonates (McKirdy et al., 1983; Peters et al., 2005b). The relatively lower value of the examined samples suggests that they belong to the carbonate facies (Table 4).

In contrast to C_{27} 18α-trisnorhopane II (Ts or 18α-22, 29, 30-trisnorhopane), Seifert and Moldowan, (1978) discovered that C_{27} 17αH-trisnorhopane (Tm or 17α-22, 29, 30-trisnorhopane) is less stable during catagenesis. Hong et al., (1986) reported that with increasing depth Tm decreases significantly compared to Ts and the relative abundance of Ts elevates systematically. At maturity levels equivalent to the earliest oil window, Tm concentrations approach zero (Hong et al., 1986; Peters et al., 2005b). The Giral mine samples have Ts/(Ts+Tm) ratio < 1, indicating the samples are immature (Table 4). Among the examined lithotypes, shales presumably have the highest ratio (average ~ 0.78) indicating the highest thermal maturity, followed by shaly lignites (average ~ 0.77) and lignites (average ~ 0.53). This is also consistent with the published T_{max} data for the studied samples (Kar et al., 2022).

C_{31} 22S/(22S+22R) can also be used to evaluate the thermal maturity of source rocks. Samples with a ratio of 0.57 to 0.62 suggest peak oil generation, whereas samples with a ratio of 0.50-0.54 indicate an early oil window stage (Peters et al., 2005b). An immature stage is indicated by an average ratio of 0.10 to 0.13 for the Giral mine samples (Table 4).

Sterane (*m/z* 217 filtered)

The tetracyclic chemical class known as sterane is produced from steroids or sterols by the catagenetic and diagenetic breakdown and saturation. Source differences may be inferred from the relative quantities of C_{27}-C_{29} steranes (Lijmbach, 1975; Roushdy et al., 2010). Ecosystems may be distinguished based on the abundance of C_{27}, C_{28} and C_{29} sterol homologs using a ternary diagram (Huang and Meinschein, 1979; Peters et al., 2005b). In contrast to higher C_{29} sterane abundance that indicates higher plant input from the terrestrial environment, higher C_{27} sterane abundance indicates an algal input with marine-lacustrine to the estuarine environment (Peters et al., 2005b; Kar et al., 2024).

The investigated lignites exhibit sterane abundance (in %) in the C_{28} and C_{29} range, indicating a predominance of higher plant deposition in a terrestrial setting (Table 4). Sterane abundance at C_{27} indicates an algal input with a marine lacustrine to estuarine environment of deposition for shaly lignites and shales. Additionally, the ternary diagram of C_{27}, C_{28} and C_{29} (in %) (Fig.12) presents two distinct organic sources- higher plants and aquatic life with dissimilar depositional environment. This identifies a shift in the distribution of OM matter and the depositional environment throughout the deposition of these three distinct lithotypes.

Repository (Table 2) presents several biomarker ratios and their global average values. These ratios are widely used to characterise source rocks to ascertain their source of OM input, depositional environment and thermal maturity.

Carbon isotope

Carbon isotope ratios in organic sediments are important to identify organic material from various land plant species and to differentiate terrestrial OM from marine sources (Rullkötter, 2001). The type and quantity of OM that shales contain directly depend on their depositional environment. Due to the variation in the isotopic composition of carbon sources, land plants exhibit distinct $\delta^{13}C$ signatures from aquatic plants (Mani et al., 2015). The organic carbon isotopic signature of lignites displays a bimodal/mixed OM input (range from -22.3 to -25.8 ‰) (Table 4). This is followed by a pseudo-bimodal distribution for shaly lignite (range from -23.3 to -25.0 ‰) and an unimodal distribution for shales (range from -24.5 to -25.0 ‰), just as the *n*-alkane distribution (Table 4).

The isotopic signatures of the various lithotypes show little fluctuation (Table 4), which may result from sediment reworking. However, the examined samples show a higher average $\delta^{13}C$ value for lignites and shaly lignites over shales. Both thermal alteration and post-depositional metamorphism can alter the $\delta^{13}C$ values. This is because of the organically lean nature of shales. Due to this, it is challenging to determine the characteristics of ^{13}C-depleted kerogen in samples to determine when it formed (Rasmussen et al., 2008; Sekine et al., 2010). However, metamorphism and thermal modification can enrich ^{13}C in OM via re-equilibration in response to the decline in the $\delta^{13}C$ value of shales (Hayes et al., 1983; Sekine et al., 2010).

Depositional environment and sea-level variation

Sedimentary basins in Rajasthan (and also Gujarat) are rifts formed due to extensional tectonics related to the fragmentation of Gondwanaland during the Mesozoic (Sharma, 2007; Singh et al., 2016). Terrestrial sediments from the Jurassic to Cretaceous Periods were first deposited in these basins, followed by sediments from the Paleocene to Eocene Epochs from marine, coastal and shallow-water environments (Sharma, 2007; Singh et al., 2016). As per Singh et al. (2019), the lignites of Gujarat and Rajasthan were produced in coastal marshy conditions during the transgression in the Paleogene, with sporadic fluvial activity resulting in a supratidal flood basin. A depositional condition with a fluctuating water level during peat deposition is suggested by a maceral investigation of the Sonari lignite mine (Kumar et al., 2020), which is located ~ 20 km SSE of the Giral mine.

Previous studies indicated marine incursion in the Barmer Basin. However, there has been a lack of research on distinguishing different lithotypes and their respective depositional environments. The current study, which investigates the depositional environment and preservation history of OM in the Giral mine, shows conclusively that the depositional environment changed between marine/aquatic to terrestrial in terms of three different lithotypes. Lignites show terrestrial oxic deposition with OM from higher terrestrial plants and marine/aquatic lower plants. Shales indicate a marine/aquatic environment with predominant marine/aquatic OM. Shaly lignites, intermediate between shales and lignites, suggest a lacustrine/estuarine environment with pseudo-bimodal OM mainly from aquatic and marine plants.

The change in depositional environment from terrestrial to marine/aquatic with altering lithology might be connected to changing sea-level conditions during the deposition of various rock types. The three rock types, shales, shaly lignites and lignites, are deposited alternately. This illustrates an episodic fluctuation in the sea level of the basin. Shales formed under marine/aquatic conditions, deposited during a high sea-level condition/marine transgression; lignites indicate a terrestrial environment of deposition formed during a low sea level or marine regression. The formation of shaly lignites, which have properties intermediate between shale and lignite, is expected during high sea level conditions. The distribution of various biomarker ratios and percentages in different lithotypes supported the aforementioned geologic situation. This places the Giral site inside a coastal environment of the continental shelf type, where episodic variations in sea-level led to the deposition of several lithotypes. A strong marine/lacustrine sulphidic reducing environment for shales and shaly lignites indicates that OM has a superior preservation history. The biologically lean character of these lithologies is attributed to a faster subsidence rate during peat deposition (Kar et al., 2022). We propose a shift in depositional conditions due to climate change. This is an important conclusion from western India, where biomarker analysis was employed to determine the shift in the depositional environment caused by periodic changes in sea-level conditions. Repository (Table 2) summarises the scope of the remaining organic geochemical analysis work for the major lignite mines in Rajasthan and Gujarat basins.

CONCLUSIONS

Based on biomarker and isotopic investigations of Eocene lignite, shales and shaly lignites from the Giral mine area of western India, the following conclusions are drawn:

- Lignites were deposited in an oxic to dysoxic terrestrial environment, with bimodal OM from terrestrial higher plants and marine/aquatic sources.
- Shales deposited exclusively in a marine/lacustrine environment with dominantly aquatic OM input.
- Shaly lignites represent an intermediate depositional environment between shales and lignites, showing a lacustrine/estuarine sequence with pseudo-bimodal OM input mainly from aquatic and marine plants.
- For shales and shaly lignites, a strongly reducing (anoxic sulphidic) environment indicates superior preservation. The physiologically lean nature of shales is due to a higher subsidence rate of the basin during peat accumulation.
- The isotopic signature reveals little variation between lithotypes, which might be due to sediment reworking.
- With the use of biomarkers, a new piece of evidence of a changing sea level linked to a variation in the depositional environment for the deposition of various lithologies is proposed for the Giral lignite mine.
- The depositional setting is linked to coastal environment, specifically those of the continental shelf type, where lithotype deposition may be influenced by periodic variations in sea level.

ACKNOWLEDGEMENTS

Funded by a seed project (RD/0120-PSUCE19-001) granted by the Center of Excellence in Oil, Gas and Energy, IIT Bombay awarded to SM. Mr. SC Sharma (Head, CEU-Lignite, Barmer) permitted to work in the Giral mine. NRK and DM thank the financial support from UoH-IoE (MHRD F11/9/2019-U3(A)). Prof. A.S. Maurya (Department of Earth Sciences, IIT Roorkee) is thanked for providing IRMS instrumentation facility for isotope analysis. Debasis Prusty assisted in generating carbon isotope data. NRK and EVSSKB thank the Director, CSIR-NGRI for permitting to submit this work. Handling Editor Bodhisatwa Hazra and anonymous reviewers are thanked for providing review comments.

Data availability

The data will be made available on request.

Conflict of Interest and Funding Sources

The authors declare no conflicts of interest. This work was supported by a seed project (RD/0120-PSUCE19-001) from the Center of Excellence in Oil, Gas, and Energy at IIT Bombay, awarded to SM. Financial assistance for NRK and DM was provided by the UoH-IoE (MHRD, F11/9/2019-U3(A)).

Repository

The repository file provides detailed information about the sample processing conducted in the lab, including solvent extraction, column chromatography, GC-MS analysis, kerogen separation, and carbon isotope analysis. Additionally, it presents a comprehensive review of various organic geochemical studies carried out in different mines within the Gujarat and Rajasthan Basin, western India (Table 1). Table 2 outlines the correlation of key biomarker ratios with global average values, while Table 3 highlights the remaining organic geochemical work for the Gujarat and Rajasthan Basin. This file also includes all the formalae for the biomarker ratios used in this study, as described in Table 3, and provides the abbreviations used in the main text.

REFERENCES

Bechtel, A., Markic, M., Sachsenhofer, R.F., Jelen, B., Gratzer, R., Lücke, A. and Püttmann, W. (2004) Paleoenvironment of the upper Oligocene Trbovlje coal seam (Slovenia). Int. J. Coal Geol. 57(1), pp.23-48. doi.org/10.1016/j.coal.2003.08.005.

Bjørlykke, K. (2015) Introduction to Petroleum Geology. In: Bjørlykke, K. (eds) Petroleum Geoscience. Springer, Berlin, Heidelberg. doi.org/10.1007/978-3-642-34132-8_1.

Bourbonniere, R.A. and Meyers, P.A. (1996) Sedimentary geolipid records of historical changes in the watersheds and productivities of Lakes Ontario and Erie. *Limnol. Oceanogr. 41*(2), pp.352-359. doi.org/10.4319/lo.1996.41.2.0352.

Chairi, R. (2018). Biomarkers on sediments in a highly saline aquatic ecosystem: case of the Moknine Continental Sebkha (Eastern Tunisia).

J. of Coast. Zone Manag. 21(2). DOI: 10.4172/2473-3350.1000463. doi:10.4172/2473-3350.1000463.

Clark, Jr, R. C. and Blumer, M. (1967) Distribution of n-paraffins in marine organisms and sediment 1. *Limnology and Oceanography, 12*(1), 79-87. DOI: https://doi.org/10.4319/lo.1967.12.1.0079

Commendatore, M.G., Nievas, M.L., Amin, O. and Esteves, J. L. (2012) Sources and distribution of aliphatic and polyaromatic hydrocarbons in coastal sediments from the Ushuaia Bay (Tierra del Fuego, Patagonia, Argentina). *Marine environmental research. 74*, 20-31. DOI: https://doi.org/10.1016/j.marenvres.2011.11.010

Directorate General of Hydrocarbons (DGH), 2018. Rajasthan Basin: Exploration and Development. [Online] Available at: https://dghindia.gov.in/assets/downloads/56ceb6e098299Rajasthan_Basin_18.pdf

Didyk, B.M., Simoniet, B.R.T. and Eglington, G. (1978) Organic geochemical indicators of paleoenvironmental conditions of sedimentation. *Nature*. 272, 216-222. DOI: https://doi.org/10.1038/272216a0

Dolson, J., Burley, S.D., Sunder, V.R., Kothari, V., Naidu, B., Whiteley, N. P. and Ananthakrishnan, B. (2015) The discovery of the Barmer Basin, Rajasthan, India, and its petroleum geology. *AAPG Bulletin*. 99(3), 433-465. DOI: https://doi.org/10.1306/10021414045

Eglinton, G. and Hamilton, R. J. (1967) Leaf Epicuticular Waxes: The waxy outer surfaces of most plants display a wide diversity of fine structure and chemical constituents. *Science*. 156(3780), 1322-1335. DOI: https://doi.org/10.1126/science.156.3780.1322

El Nemr, A., Moneer, A.A., Ragab, S. and El Sikaily, A. (2016) Distribution and sources of n-alkanes and polycyclic aromatic hydrocarbons in shellfish of the Egyptian Red Sea coast. *Egyptian Journal of Aquatic Research. 42*(2), 121-131. DOI: https://doi.org/10.1016/j.ejar.2016.05.003

Farrimond, P., Naidu, B.S., Burley, S.D., Dolson, J., Whiteley, N. and Kothari, V. (2015) Geochemical characterization of oils and their source rocks in the Barmer Basin, Rajasthan, India. *Petroleum Geoscience*. 21 (4): 301–321. DOI: https://doi.org/10.1144/petgeo2014-075

Ficken, K.J., Li, B., Swain, D.L. and Eglinton, G. (2000) An n-alkane proxy for the sedimentary input of submerged/floating freshwater aquatic macrophytes. *Organic geochemistry,* 31(7-8), 745-749. DOI: https://doi.org/10.1016/S0146-6380(00)00081-4

Gearing, P., Gearing, J.N., Lytle, T.F. and Lytle, J. S. (1976) Hydrocarbons in 60 northeast Gulf of Mexico shelf sediments: a preliminary survey. *Geochimica et Cosmochimica Acta*. 40(9), 1005-1017. DOI: https://doi.org/10.1016/0016-7037(76)90043-0

Gelpi, E., Schneider, H., Mann, J. and Oro, J. (1970) Hydrocarbons of geochemical significance in microscopic algae. *Phytochemistry*. 9(3), 603-612. DOI: https://doi.org/10.1016/S0031-9422(00)85700-3

Hayes, J. M., Kaplan, I.R. and Wedeking, K.W. (1983) Precambrian organic geochemistry, preservation of the record, in The Earth's Earliest Biosphere: Its Origin and Evolution, edited by J W Schopf pp. 93–34; *Princeton Univ.* Press Princeton, N. J.

Henrichs, S.M. (1993) Early Diagenesis of Organic Matter: The Dynamics (Rates) of Cycling of Organic Compounds. In: Engel, M.H., Macko, S.A. (eds) Organic Geochemistry. Topics in Geobiology, vol 11. Springer, Boston, MA. DOI: https://doi.org/10.1007/978-1-4615-2890-6_4

Zhi-Hua, H., Hui-Xiang, L., Rullkötter, J. and Mackenzie, A.S. (1986) Geochemical application of sterane and triterpane biological marker compounds in the Linyi Basin. *Organic geochemistry*. 10(1-3), 433-439. DOI: https://doi.org/10.1016/0146-6380(86)90043-4

Huang W.Y. and Meinschein W.G. (1979) Sterols as ecological indicators. *Geochimica et Cosmochimica Acta. 43*(5), 739-745, ISSN 0016-7037. DOI: https://doi.org/10.1016/0016-7037(79)90257-6.

Hunt, J. M. (1995) Petroleum Geology and Geochemistry; W. H. *Freeman and Company, San Francisco*, 617, ISBN: 0716724413.

Kar, N.R., Mani, D., Mukherjee, S., Dasgupta, S., Puniya, M.K., Kaushik, A.K. and Babu, E.V.S.S.K. (2022) Source rock properties and kerogen decomposition kinetics of Eocene shales from petroliferous Barmer basin, western Rajasthan, India. *Journal of Natural Gas Science and Engineering. 100* 104497. DOI: https://doi.org/10.1016/j.jngse.2022.104497

Kar, N.R., Mani, D. and Babu, E.V.S.S.K. (2024) Tracing the Late Permian Gondwana surface environments using sedimentary biomarkers from the Raniganj Formation, Damodar Valley, Eastern India. *Journal of Sedimentary Environments*. 1-24. DOI: https://doi.org/10.1007/s43217-024-00192-8

Kumar, A., Hakimi, M.H., Singh, A.K., Abdullah, W.H., Zainal Abidin, N.S., Rahim, A. and Yelwa, N.A. (2022) Geochemical and petrological characterization of the early Eocene carbonaceous shales: Implications for oil and gas exploration in the Barmer Basin, Northwest India. *ACS omega*. 7(47), 42960-42974. DOI: 10.1021/acsomega.2c05148

Kumar, A., Singh, A.K., Paul, D. and Kumar, A. (2020) Evaluation of hydrocarbon potential with insight into climate and environment present during deposition of the Sonari lignite, Barmer Basin Rajasthan. *Energy and Climate Change*. 1, 100006. DOI: https://doi.org/10.1016/j.egycc.2020.100006

Lijmbach, G.M.G. (1975) On the origin of petroleum. In 9th World Petroleum Congress, Proc. (Vol. 2, pp. 357-369). Appled Science Publishers.

Mani, D., Kar, N.R. and Kalpana, M.S. (2022) Source Rock Geochemistry for Shale Characterization. *Handbook of Petroleum Geoscience: Exploration, Characterization, and Exploitation of Hydrocarbon Reservoirs.* 233-253, Wiley Publication. ISBN: 978-1-119-68003-1.

Mani, D. and Kar, N.R. (2024) Emerging Techniques for Evaluating Thermal Maturity in Shale Gas Systems. *Unconventional Shale Gas Exploration and Exploitation: Current Trends in Shale Gas Exploitation*. 1-13. DOI: http://dx.doi.org/10.1007/978-3-031-48727-9_1

Mani, D., Patil, D.J., Dayal, A.M. and Prasad, B.N. (2015) Thermal maturity, source rock potential and kinetics of hydrocarbon generation in Permian shales from the Damodar Valley basin, Eastern India. *Mar. Petrol. Geol. 66*, 1056–1072. DOI: https://doi.org/10.1016/j.marpetgeo.2015.08.019

McKirdy, D.M., Aldridge, A.K. and Ypma, P.J.M. (1983) A geochemical comparison of some crude oils from Pre-Ordovician carbonate rocks; *In: Advances in Organic Geochemistry 1981 (M. Bjorøy, C. Albrecht, C. Cornford, et al., eds.), John Wiley & Sons, New York*, pp. 99–107.

Oldham, R.D. (1886) Geology of northern Jaisalmer. *Record Geol. Surv. India. 19*, 157–159.

Ourisson, G., Albrecht, P. and Rohmer, M. (1979) The hopanoids. Palaeochemistry and biochemistry of a group of natural products. *Pure and Applied Chemistry*. 51, 709–29.

Peters, K.E., Walters, C.C. and Moldowan, J.M. (2005a) The biomarker guide: biomarkers and isotopes in the environment and human history. *Cambridge University Press, Cambridge, UK*. ISBN: 0 521 78158 2

Peters, K.E., Walters, C.C. and Moldowan, J.M. (2005b) The Biomarker Guide, Volume 2: Biomarkers and Isotopes in the Petroleum Exploration and Earth History. *Cambridge University Press, Cambridge, UK*. ISBN: 0 521 83762 6

Powell, T.G. (1984) Developments in concept of hydrocarbon generation from terrestrial organic matter. *Beijing Petroleum Symposium (20-24 Sept. 1984) Beijing, China.*

Prasad, V., Uddandam, P.R., Agrawal, S., Bajpai, S., Mishra, I.S.A.K., Sharma, A. and Verma, M.K.P. (2020) Biostratigraphy, palaeoenvironment and sea level changes during pre-collisional (Palaeocene) phase of the Indian plate: palynological evidence from Akli Formation in Giral Lignite Mine, Barmer Basin, Rajasthan, Western India. *Episodes Journal of International Geoscience*. 43, 476-488. DOI: https://doi.org/10.18814/epiiugs/2020/020030

Punyu, V.R., Hariji, R.R., Bhosle, N.B., Sawant, S.S. and Venkat, K. (2013) n-Alkanes in surficial sediments of Visakhapatnam harbour, east coast of India. *J. Earth Syst*. Sci. 122, 467–477. DOI: https://doi.org/10.1007/s12040-013-0268-0

Raju, S.V. and Mathur, N. (2013) Rajasthan lignite as a source of unconventional oil. *Curr*. Sci. 104, 752–757.

Rasmussen, B., Fletcher, I.R., Brocks, J.J., and Kilburn, M.R. (2008) Reassessing the first appearance of eukaryotes and cyanobacteria. *Nature*. 455, 1101–1104. DOI: https://doi.org/10.1038/nature07381

Roushdy, M.I., El Nady, M.M., Mostafa, Y.M., El Gendy, N.S. and Ali, H.R. (2010) Biomarkers characteristics of crude oils from some oilfields in the Gulf of Suez, Egypt. *Journal of American Science. 6*, 911-925.

Roy, A.B. and Jakhar, S.R. (2002) Geology of Rajasthan (Northwest India) Precambrian to Recent; *Scientific Publishers, Jodhpur*, pp. 1–421.

Rullkötter, J. (2001) Geochemistry, organic. Encyclopedia of Physical Science and Technology, 3rd edition: Academic Press, San Diego, 6, 549-574.

Scalan, E. S. and Smith, J. E. (1970) An improved measure of the odd-even predominance in the normal alkanes of sediment extracts and petroleum. *Geochimica et cosmochimica acta. 34*(5), 611-620. DOI: https://doi.org/10.1016/0016-7037(70)90019-0

Seifert, W. K. and Moldowan, J. M. (1978) Applications of steranes, terpanes and monoaromatics to the maturation, migration and source of crude oils. *Geochimica et cosmochimica acta. 42*(1), 77-95. DOI: https://doi.org/10.1016/0016-7037(78)90219-3

Sekine, Y., Tajika, E., Ohkouchi, N., Ogawa, N.O., Goto, K., Tada, R. and Kirschvink, J. L. (2010) Anomalous negative excursion of carbon isotope in organic carbon after the last Paleoproterozoic glaciation in North America. *Geochemistry, Geophysics, Geosystems*. 11(8). DOI: https://doi.org/10.1029/2010GC003210

Sharma, K.K. (2007) K-T magmatism and basin tectonism in western Rajasthan, India, results from extensional tectonics and not from reunion plume activity. Foulger GR, Jurdy DM (eds), Plates, plumes and planetary processes; *Geological Society of America Special Paper. 430*, 775–784.

Singh, P.K., Rajak, P.K., Singh, M.P., Naik, A.S., Singh, V.K., Raju, S.V. and Ojha, S. (2015) Environmental Geochemistry of selected elements in lignite from Barsingsar and Gurha Mines of Rajasthan, Western India. *Journal of the Geological Society of India. 86*, 23-32. DOI: https://doi.org/10.1007/s12594-015-0277-5

Singh, P.K., Rajak, P.K., Singh, M.P., Singh, V.K., Naik, A.S. and Singh, A. K. (2016) Peat swamps at Giral lignite field of Barmer basin, Rajasthan, Western India: understanding the evolution through petrological modelling. *International Journal of Coal Science & Technology. 3*, 148-164. DOI: https://doi.org/10.1007/s40789-016-0137-y

Singh, V.K., Rajak, P.K. and Singh, P.K. (2019) Revisiting the paleomires of western India: An insight into the early Paleogene lignite Corridor. *Journal of Asian Earth Sciences. 171*, 363-375. DOI: https://doi.org/10.1016/j.jseaes.2018.08.031

Stefanova, M., Oros, D.R., Otto, A. and Simoneit, B.R. (2002) Polar aromatic biomarkers in the Miocene Maritza-East lignite, Bulgaria. *Organic Geochemistry. 33*(9), 1079-1091. DOI: https://doi.org/10.1016/S0146-6380(02)00084-0

Tewari, A., Dutta, S. and Sarkar, T. (2017) Biomarker signatures of Permian Gondwana coals from India and their palaeobotanical significance. *Palaeogeography, Palaeoclimatology, Palaeoecology. 468*, 414-426. DOI: https://doi.org/10.1016/j.palaeo.2016.12.014

Nihar Ranjan Kar is a Senior Technical Officer at CSIR-NGRI and is pursuing PhD from the University of Hyderabad. He specializes in organic geochemistry, fuel geology, and petroleum system studies. He was involved in fieldwork, sample preparation, data interpretation and preparation of the manuscript.

Bala Subramanyam Seetha is a Postdoctoral researcher at Stockholm University. He is a mass spectrometrist, having expertise in handling GC-MS/MS instrument. He was involved in GC-MS analysis to generate biomarker data.

Devleena Mani Tiwari is an Assistant Professor at the Centre for Earth, Ocean and Atmospheric Sciences, University of Hyderabad. Her research focuses on natural resource exploration and paleoclimatic reconstructions using organic and isotope geochemistry. She contributed to the generation and interpretation of biomarker data and manuscript preparation.

EVSSK Babu is a Chief Scientist, Project Leader and Head, Geochronology and Isotope Studies Group, CSIR-NGRI and Professor of Physical Sciences at the AcSIR. He is a multidisciplinary Earth Scientist with vast expertise in *in-situ* elemental and isotopic analyses. He was involved in drafting the manuscript.

Soumyajit Mukherjee is a Professor at IIT Bombay. Expertise in structural geology and tectonics. He was involved in the fieldwork and preparation of the manuscript.

Mohana Krishna Reddy Mudiam is the Director of the Institute of Pesticide Formulation Technology. He specializes in analytical chemistry, chemometrics, organic chemistry and biochemistry. He was involved in the GC-MS analysis of biomarker compounds.

Swagato Dasgupta is a production seismologist and geoscientist. He specializes in tectonics, seismic analysis, and reservoir modeling. He assisted with fieldwork and sample collection.

Handling Editor: Bodhisatwa Hazra

Supplementary material for the article "Biomarker Evidence of Shifts in Organic Provenance and Depositional Environments of Eocene Carbonaceous Rocks from Petroliferous Barmer Basin, Western Rajasthan, India" by Nihar Ranjan Kar, Devleena Mani, Bala Subrahanyam Seetha, E.V.S.S.K. Babu, Soumyajit Mukherjee, Swagato Dasgupta and Mohana Krishna Reddy Mudiam. Jour. Geol. Soc. India, v.101, pp. 112-122.

REPOSITORY MATERIALS

Repository Table 1. A review of different organic geochemical works carried out in the various mines from Gujarat and Rajasthan Basins, western India.

Sl. No.	Author(s)	Mine	Techniques	Key conclusions
1	Mukherjee et al. (1992)	Kapurdi lignite mine, Barmer Basin, Rajasthan, India	Petrography, proximate & ultimate analysis	*(i)* Lignites are are rich in huminite macerals followed by liptinite and negligible inertinite. *(ii)* Three significant lignite-bearing bands marked with a significant variation in lithofacies over a short distance. The lignites are mature and have a low ash content. *(iii)* Compared to the lignites, which have moderate fusion temperatures, carbonaceous beds are extremely refractory and siliceous in composition.
2	Dutta et al. (2009)	Resins from Tadkeshwar, Cambay Basin; Panandhro, Kutch Basin; Neyveli, Cauvery Basin, India.	Ultimate analysis, Fourier Transform Infrared Spectroscopy (FTIR), biomarker analysis	*(i)* The examined resins are classified as Class II/dammar resins. These are suitable for exploration purposes. *(ii)* The occurrence of these resins is identified as either from Dipterocarpaceae or from other angiosperms. *(iii)* If Dipterocarpaceae is responsible for such fossil resin occurrences, this would be an expansion of their first presence in India during the Eocene epoch.
3	Mallick et al. (2009)	Eocene Resin, Vastan lignite mine, Cambay Basin, Gujarat, India	Ultimate analysis, FTIR, biomarker analysis	*(i)* The resins are classified as Class II resins. *(ii)* The resins are made from dammar resins found in several angiosperm species. *(iii)* A terrestrial input with a tropical forest climatic condition recorded for the deposition of these resins.
4	Singh et al. (2010)	Vastan lignite mines, Gujarat, India	Petrography, proximate & ultimate analysis	*(i)* The lignites are rich in huminite group of macerals. *(ii)* These lignites are rich in moisture content, moderate to high volatile matter, and have a variable ash content. Carbonates and sulphides are present in lesser concentration. *(iii)* The OM deposited in a reducing environment with high anaerobic activity.
5	Dutta et al. (2011)	Matanomadh lignites, Kutch basin, western India	Organic petrology, palynology, elemental analysis, rock-eval pyrolysis, FTIR, biomarker analysis	*(i)* The OM supply, for Matanomadh lignites, was mostly dominated by angiosperm woody forest vegetation. The OM attained an early diagenetic stage of methane generation thermal maturity. *(ii)* The depositional environment was tropical to sub-tropical with proximity to the paleo-shoreline. *(iii)* Appearance of the Dipterocarpaceae family plants during the Eocene Epoch is reported for the Indian continent.
6	Singh (2012)	Rajpardi & Palana lignites, Gujarat, India	Petrography, proximate & ultimate analysis, huminite reflectance	*(i)* The examined lignites are of low-rank B coal and rich in huminite macerals. *(ii)* The lignites are per-hydrous and possess a higher conversion factor for the liquefaction process. *(iii)* In Rajpardi lignite, the O/C and H/C ratios decrease as the rank increases, but in Vastan lignite, the opposite applies.
7	Singh et al. (2012)	Rajpardi lignites, Gujurat, India	Petrography, proximate & ultimate analysis, huminite reflectance	*(i)* Rajpardi lignites are low rank-B coals with higher volatile matter and hydrogen content. The mineral matter present is mostly composed of argillaceous minerals, followed by carbonate with pyrite in trace amounts. *(ii)* The OM is rich in huminite maceral, with a depositional habitat ranging from limno-telmatic forest swamps to telmatic forest swamps. An increased subsidence rate reported for the preservation of maceral structure. *(iii)* Rajpardi lignite, a novel facies mode proposed, formed in a forest swamp under wet moor settings with moderate to high flooding, good tissue preservation, and growing bacterial activity.
8	Kumar et al. (2013)	Panandhro lignite mine, Kutch Basin, Gujarat, India	Huminite reflectance	*(i)* Lignites are at the brown coal stage. *(ii)* The lignites have attained an early diagenetic methane generation stage. (iii) Block-4 of the Panandhro lignite mine has been identified as an appropriate fuel for the steam generation process.

Repository Table 1 continued…

Sl. No.	Author(s)	Mine	Techniques	Key conclusions
9	Mishra et al. (2014)	Shales from Mata-no-Madh, Panandhro lignite mines and Umarsar region, Kutch Basin, Gujarat, India	Rock-Eval pyrolysis	*(i)* Shales are organically rich and have a higher potential for generating gaseous hydrocarbon. *(ii)* The OM input is from Type II-III kerogen and is mostly immature. *(iii)* The deeper investigation of these shales can precisely define the horizons for gas plays.
10	Paul et al. (2015)	Surkha lignite mine, Cambay basin, western India	Rock-Eval pyrolysis, biomarker, palynology, organic petrography	*(i)* The age for low-rank B Surkha lignites is assigned to be of the Early Eocene from the palynological study. *(ii)* The OM input is rich in liptinite maceral and at an immature stage. *(iii)* Hot humid tropical conditions prevailed during the Early Eocene time. *(iv)* Marginal marine depositional setting marked with intermediate marine incursion to the basin.
11	Singh et al. (2015)	Barsingsar and Gurha mines, Rajasthan, western India	Petrography, proximate analysis, trace element distribution	*(i)* For Barsingsar the concentrations of Ni, Co and Pb is 4-5 times higher while the Cd is 10-20 times higher than the Clarke values. Similarly for Gurha lignites the concentration of Co, Cu and Ni is 2-4 times while Cd is 5-10 times higher than the Clarke values. *(ii)* Marine incursion reported during peat formation for both the mines. *(iii)* In Barsinghsar lignites, the Ca and Mg elements got enriched during the humification process, as shown by their stronger affinity toward OM, whereas the Cu, Co, K, Pb enriched from the inorganic sources.
12	Paul and Dutta (2016)	Resins from Giral mine, Barmer Basin and Gurha mine, Bikaner-Nagaur Basin, Rajasthan, India	Rock-Eval pyrolysis, biomarker analysis	*(i)* The resins are identified to have predominant gymnosperm derived diterpenoids. The angiosperm derived triterpenoids are absent. *(ii)* The study revealed, in India, Early Paleogene resins were not only represented by fossil dammars from the Dipterocarpaceae family of angiosperm; some of them were also formed from conifers. *(iii)* An oxic depositional condition marked for the Barmer Basin.
13	Singh et al. (2016)	Giral lignite mine, Barmer basin, Rajasthan, western India	Petrography, proximate & ultimate analysis, rock-eval pyrolysis	*(i)* The OM is rich in huminite maceral with moderate to low ash yield. The lignites are of low-rank C coal, mostly at the immature stage. *(ii)* The presence of megascopic resin and specks of pyrite reported in the stratified black bands within the lignite seams. *(iii)* Barmer lignites formed mostly in wet forest wetland to clastic marsh environments with telmatic to limno-telmatic conditions with a slow decline in groundwater table and moderate subsidence rate. *(iv)* The somewhat high calcium content, as well as the occurrence of framboidal pyrite, point to increased sulphate-reducing microbial action in the basin's carbonate and sulphate-rich waters during peat formation.
14	Singh et al. (2016)	Lignites of Barsingsar, Gurha, and Kasnau-Matasukh mine, Bikaner-Nagaur basin, Rajasthan, India	Petrography, proximate & ultimate analysis, rock-eval pyrolysis	*(i)* The OM supply for these lignites is mostly from Type-III kerogen dominant with huminite macerals. *(ii)* The lignites have low-medium ash yield with a higher volatile matter. *(iii)* The fixed hydrocarbon is significantly higher than the free hydrocarbon. *(iv)* Study supports the lignites are suitable for artificial conversion or liquefaction process.
15	Singh et al. (2016)	Lignites of Vastan, Rajpardi and Tadkeshwar, Gujurat, India	Petrography, proximate & ultimate analysis, rock-eval pyrolysis	*(i)* The lignites are determined to be of low rank C coal and are rich in Huminite maceral. *(ii)* The study investigates an immaturity of OM and an input mostly from Type III kerogen with minor inputs from Type II. *(iii)* The lignites are rich in volatile matter, a variable ash content and a moderate sulfur content. Tadkeshwar lignites are examined to be sub-hydrous, whereas Rajpardi lignites are perhydrous. Vastan lignites are examined to be bright coal category. *(iv)* The lignites are examined to be suitable source rock for HC generation and have a greater conversion rate and oil yield.
16	Kumar et al. (2017)	Cambay Shale, Cambay Basin, Gujarat, India	Loss of ignition, TOC analysis, rock-eval pyrolysis, organic petrography	*(i)* Cambay shales represent an OM input from Type II-III kerogen. The shales are matured enough to reach their oil generation stage, but the peak oil stage and gas generation stage are not yet reached. *(ii)* Seven organic-rich rock bands, varying thickness between 3-30m, were examined to have a fair to good OM content as well as hydrocarbon generating potential. *(iii)* A 30 m thick sequence examined at a depth below 1954 m was found to be an excellent source rock and might be a sweet spot for shale oil. *(iv)* Along with the source rock characterization, the study points out few potential resource horizons. It also offered a low risk in obtaining the predicted reserve.

Repository Table 1 continued…

Sl. No.	Author(s)	Mine	Techniques	Key conclusions
17	Singh et al. (2017)	Matasukh lignite mine, Bikaner-Nagaur basin, western India	Petrography, palynofacies & palynology, biomarker	*(i)* Low-rank B lignites, rich in terrestrial OM indicated by huminite macerals. *(ii)* The OM has undergone a certain stage of bacterial degradation. An environmental transition between suboxic-anoxic marked by the p5alynofacies fluctuations. *(iii)* The environmental shift found from hinterland rainforest vegetation to Early Eocene warm/humid tropical-subtropical climatic conditions with higher precipitation.
18	Singh et al. (2017)	Matasukh lignite mine, Nagaur Basin, western Rajasthan, India	Petrography, proximate analysis, huminite reflectance	*(i)* Matasukh lignites of low-rank B coals, and are rich in huminite group of macerals. *(ii)* The OM input is mostly from Type-III kerogen. These kerogens are capable of producing gas only. *(iii)* A marshy environment is proposed for the accumulation of peat. *(iv)* The OM deposited in a mildly oxic to anoxic with a changing groundwater level condition between ombrotrophic to mesotrophic. A predominant bacterial activity with some sort of marine intercalation is also marked during the deposition of OM.
19	Singh et al. (2017)	Surkha lignite mines, Bhavnagar, Saurashtra Basin, Gujarat, India	Petrography, proximate & ultimate analysis, huminite reflectance	*(i)* Saurashtra lignites are rich in Huminite macerals and deposited in a wet moor environment with a low tissue preservation condition. *(ii)* A low subsidence rate, rheotrophic hydrological condition and shift in environment between limnic to telmatic to again limnic encountered while deposition of these lignites. The presence of Framboid pyrites revealed a marine influence to the basin. *(iii)* The upper seam shows a higher bacterial degradation than of lower seam. Also, dried periods were found during the deposition of the lower seam. *(iv)* The lignites are examined to have excellent hydrocarbon generating potential.
20	Singh et al. (2017)	Lignites from Surkha lignite mine, Saurashtra Basin, Gujarat, India	Petrography, palynofacies analysis, proximate & ultimate analysis, gross calorific values, rock-eval pyrolysis, biomarker analysis	*(i)* The examined lignites are rich in huminite maceral suggesting OM input from woody forest. A type II-III OM input both from gymnosperm and angiosperm higher plants recorded. The OM is examined to be immature. *(ii)* The lignites are rich in moisture, volatile matter, carbon and oxygen level, with a low-moderate sulfur content and a low ash yield. *(iii)* The lignites were deposited in a deltaic setting with changing hydrological conditions, limno-telmatic source vegetation, and dysoxic-anoxic conditions. Bacterial activity accumulated in OM as well. *(iv)* The OM is examined to be suitable for the production of both oil and gas.
21	Mathews et al. (2018)	Panandhro lignites, Kutch basin, western India	Ultimate analysis, FTIR, rock-eval pyrolysis, palynology	*(i)* Panandhro lignites deposited under a humid tropical climate, with OM mostly coming from an angiosperm-dominated mixed forest ecosystem. *(ii)* Immature OM with Type II-III admixed kerogen input. *(iii)* The presence of dinoflagellate cysts and mangrove pollen with moderate sulfur content marks nearshore or marine-influenced depositional setting.
22	Rajak et al. (2018)	Giral lignites, Barmer Basin, Rajasthan, India	Petrographic analysis, proximate & ultimate analysis, rock-eval pyrolysis, X-ray diffraction (XRD), FTIR, Scanning Electron Microscopy-Energy Dispersive X-ray Spectroscopy (SEM-EDS), elemental and mineral matter analysis	*(i)* Detrital or terrigenous origin marked for Giral lignites. *(ii)* The lignites have a medium-high sulfur content with higher mineral carbon towards the middle seam. The presence of kaolinite, silicate, sulphides and clay minerals are reported. *(iii)* Cd, Ni, Na, K and Pb show a higher concentration. This indicates the potential threat to the environment. To protect the environment, prior chemical or microbiological treatment is suggested before using these rocks for our purposes.
23	Singh et al. (2018)	Gurha lignites, Bikaner basin, Rajasthan, India	Petrography, proximate & ultimate analysis, rock-eval pyrolysis, huminite reflectance	*(i)* The Gurha lignites are dominated by huminite group of macerals. The maceral investigation identified the proportional degree of deterioration and breakdown of the primary peat material. *(ii)* The lignites are of low rank-B and mostly immature. The OM input examined to be of Type-III kerogen, mostly from herbaceous plants in forest swamp conditions. Study finds these samples can generate both oil and gas (mostly gas) upon maturation. *(iii)* The OM was deposited in a wet moor with moderate flooding and growing bacterial activity, as well as in a bog forest with ombrotrophic hydrological conditions. A marine incursion activity reported during the deposition of these lignites.

Repository Table 1 continued…

Sl. No.	Author(s)	Mine	Techniques	Key conclusions
24	Singh et al. (2018)	Matasukh mine, Nagaur Basin, western Rajasthan, India	Petrography, proximate & ultimate analysis, rock-eval pyrolysis, huminite reflectance	*(i)* Some of the Matasukh lignites are rich in liptinite maceral, whereas other coals rich in huminite group maceral. The OM input examined to be both Type II-III (mixed type) kerogen. This suggests the OM is suitable for generating both liquid and gaseous hydrocarbons upon maturation. *(ii)* The OM is immature and coal type ranging between lignite to the sub-bituminous stage. *(iii)* The OM is rich in moisture, volatile matter and have a low fixed carbon concentration. *(iv)* The study indicates that these coals are suitable for forming various hydrocarbon products by thermal cracking.
25	Singh and Kumar (2018)	Matasukh lignite mine, Nagaur Basin, western Rajasthan, India	Petrography, rock-eval pyrolysis, biomarker analysis, huminite reflectance	*(i)* Matasukh lignites are of low-rank B coals and are thermally immature. *(ii)* A terrigenous to mixed OM input specifically from conifers and angiosperm marked for the region. *(iii)* An anoxic depositional environment was prevailing for the deposition of OM.
26	Srivastava et al. (2018)	Black shales from Kutch, Gujarat, India	Rock-Eval pyrolysis, SEM	*(i)* The upper Jurassic Jhuran Formation is identified as organically lean, Type-IV inert kerogen, deposited in a marine environment. *(ii)* The organically lean nature could be due to the over-maturation of OM either by oxidative weathering or Deccan Trap volcanism. *(iii)* The Early Eocene Naredi Formation black shales are organically rich, immature Type III-IV kerogen, deposited in a reducing swampy type environment. These shales are identified as good for generating coal or gas after maturation.
27	Kumar et al. (2022)	Giral lignites, western Rajasthan, India	Proximate & ultimate analysis, isolation and screening of native microorganisms, microbial desulfurization of lignite, SEM-EDS, XRD, FTIR	*(i)* Giral lignites are sulfur-rich and have a low ash yield. *(ii)* Burkholderia sp. was used for the desulfurization process. *(iii)* The chemical treatment resulted in a relative reduction in the ash yield and volatile matter; with an increase in the percent of elemental carbon and fixed carbon. *(iv)* The significant increase in the gross calorific value of lignites following this chemical treatment demonstrates that this approach has the potential to create clean fuel from this location.
28	Prasad et al. (2020)	Giral lignite mine, Barmer Basin, Rajasthan, India	Palynological study, carbon isotope analysis	*(i)* In contrast to earlier workers the age of the Giral lignite mine is determined as Danian-Thanetian. *(ii)* Two eustatic maximum flooding surfaces marked at 60.7 Ma and 57.9 Ma, *(iii)* A complete sequence stratigraphic study has been done for Giral mines with the help of palynological and isotope studies. Five different depositional units, deposited in a changing sea-level condition between the transgressive system tract and high stand system tract, have been identified for the Giral lignite mine.
29	Rajak et al. (2019)	Lignite samples from Vastan, Rajpardi and Tadkeshwar mines of Cambay Basin, Bhavnagar-Surkha mine of Saurashtra basin, Matamomadh and Panandhro mines of Kutch basin, Gujarat. Barsingsar, Gurha, Kasnau-Matasukh mines of Bikaner-Nagaur Basin, Giral and Kapurdi mines of Barmer Basin, Rajasthan, India.	Petrographic analysis	*(i)* The lignites are rich in Huminite maceral followed by liptinite and less inertinite. *(ii)* Local to regional scale wildfires recorded for the Gujarat and Rajasthan area. *(iii)* The charcoal content of the Early Paleogene wildfire activities compares favourably with that of other sections of the world.
30	Singh and Kumar (2020)	Barsingsar mine, Bikaner–Nagaur Basin, western Rajasthan, India	Petrography, proximate & ultimate analysis, rock-eval pyrolysis, huminite reflectance, XRD, X-ray fluorescence (XRF), FTIR	*(i)* The Barsingsar lignites are rich in huminite group of macerals followed by inertinite. These are rich in mineral matter and have a low sulfur content. *(ii)* The OM input found to be from both Type II-III kerogen and at their immature stage. *(iii)* The lignites are rich in kaolinite, marcasite and other oxides such as siderite, quartz, rutile, aragonite and coesite. *(iv)* A dry/oxic environment documented during the peat accumulation. The presence of a fluvial high-energy environment was recorded. Organic matter deposited in a deltaic environment in sub-oxic to oxic conditions.

Repository Table 1 continued…

Sl. No.	Author(s)	Mine	Techniques	Key conclusions
31	Singh et al. (2020)	Umarsar lignites, Kutch, Gujarat, India	Maceral study, proximate & ultimate analysis, rock-eval pyrolysis, huminite reflectance	*(i)* The Umarsar lignites are organically rich and have a higher hydrocarbon generation potential. *(ii)* The OM input is governed by Type II-III kerogen and is mostly immature. *(iii)* The lignites examined have a greater generation potential to generate both oil and gas.
32	Singh et al. (2019)	Paleogene lignites, western India	Compilation of petrographic, palynologic and geochemical data from different lignite-bearing sequences of Rajasthan and Gujarat	*(i)* The lignites of western India is mostly rich in huminite group of macerals with OM input mostly from herbaceous and marginal marine plants. *(ii)* The OM deposited in a relatively wet condition, tropical to sub-tropical climate, with a slow subsidence rate of the basin. Some intermediate period of oxic environment also reported from some area. *(iii)* A mesotrophic to rheotrophic groundwater condition persisted during the deposition of OM. *(iv)* The development of lignites in Gujarat and Rajasthan during the transgression phase occurred in a coastal marshy environment that was sporadically affected by fluvial activity events.
33	Kumar et al. (2020)	Sonari lignite, Barmer basin, Rajasthan	Petrography, bulk rock analysis using rock-eval, biomarker, stable carbon isotope, FT-IR and Nuclear Magnetic Resonance (NMR) study	*(i)* Thermally immature low-reflecting lignite, b in rank. But the lignites have an excellent source rock potential. *(ii)* Dominant Type-III kerogen rich in huminite maceral. *(iii)* OM input mostly from gymnosperms under a cool and dry conditions.
34	Mathews et al. (2020)	Gurha lignites, Bikaner basin, Rajasthan, India	Petrography, palynology, palynofacies, rock-eval pyrolysis, biomarker analysis	*(i)* The OM input for these rank B lignites mostly indicates a terrigenous higher plant input, evolved in a mostly tropical-subtropical to temperate climatic condition. *(ii)* The OM deposited in a limno-telmatic condition with fluctuating water table. A shift in the depositional environment from oxic-dysoxic to suboxic-anoxic marked. *(iii)* Samples are mostly immature but have an excellent potential to generate different hydrocarbon products upon maturation.
35	Mathews et al. (2020)	Barsingsar lignites, Bikaner–Nagaur Basin, Rajasthan, India	Biomarker analysis, TOC, $\delta^{13}C$	*(i)* A significant climatic variation persisted during the deposition of the lignite-bearing sequence. *(ii)* The climatic shift in that location caused a shift in OM contribution from terrestrial to marine and changes in OM characteristics.
36	Rajak et al. (2020)	Kapurdi lignites, Barmer Basin, Rajasthan, western India	Petrographic analysis, proximate & ultimate analysis, rock-eval pyrolysis, XRD, FTIR, SEM-EDS, trace element analysis	*(i)* The Kapurdi lignites have a low-inorganic, low-mineral content and a medium-high sulfur concentration. *(ii)* A detrital terrigenous input to the basin. The lignites are constitutes of silicate, illite, kaolinite, hematite and other clay minerals. *(iii)* The concentration of environmental sensitive elements such as Ni, Pb, Na, Co, Cd and K are found to be higher than the Clarke value. Hence a suitable means of beneficiation is required, before its utilization, to protect the environment.
37	Singh et al. (2020)	Gurha mine, Rajasthan, Bikaner basin, NW India	Petrography, bulk rock analysis using rock-eval, ultimate analysis, biomarker analysis	*(i)* A superior preservation of the OM under a reducing condition as examined by the higher TOC and TS content for shales. *(ii)* Dominant marine algae contribution than of freshwater algae. *(iii)* Type II kerogen input mostly from marine phytoplankton algae for the examined bituminous shales indicates a better oil-shale resource. *(iv)* The OM is immature, hence can be looked for artificial conversion into different hydrocarbon products using artificial techniques.
38	Choudhury et al. (2021)	Glauconites of Giral Member, Barmer basin, western India	Petrography, XRD, major oxide using Electron Probe Microanalyzer (EPMA)	*(i)* The Eocene lignites of Giral Member support a marine flooding event with a combination of freshwater inflow and higher sedimentation rate. *(ii)* Glauconitization was facilitated during the Early Eocene due to the prevalence of the warm climatic condition. *(iii)* Glauconite precipitation during the Early Eocene might be one of the causes for Fe sinking in a shallow, marginal coastal depositional environment.
39	Das et al. (2021)	Permian coals from East Sikkim, Cenozoic coals from Arunachal Pradesh, Assam, Tamil Nadu, Tadkeshwar and Panandhro lignite mines, Gujarat, India	Total nitrogen, total carbon, stable isotope analysis, rock-eval pyrolysis	*(i)* The examined Cenozoic coals are immature and have a predominant OM input mostly from type III to type II-III kerogen. These Cenozoic coals originated from an angiosperm-dominated source, while Permian coals came from a gymnosperm-dominated source. *(ii)* Permian coals shows a δ13C enrichment in comparison to Cenozoic coals. Enrichment occurs as a result of the accumulation of heavier carbon isotopes during coalification. *(iii)* Coalification and tectonic activity have almost no effect on the source signatures of carbon isotopes.

Repository Table 1 continued…

Sl. No.	Author(s)	Mine	Techniques	Key conclusions
40	Hakimi et al. (2023)	Kapurdi mine, Barmer Basin, Rajasthan, India	Total Organic Carbon (TOC) & Total Sulphur (TS) analysis, rock-eval pyrolysis, ultimate analysis, pyrolysis-gas chromatography, biomarker analysis, petrography, huminite reflectance	*(i)* The examined bituminite shales are rich in organic matter and are excellent source rock for hydrocarbon generation. *(ii)* The OM input governed from the oil-prone kerogen, and mostly immature. *(iii)* A non-marine lacustrine-type depositional environment proposed for the deposition of OM. *(iv)* The bituminite shales are identified as a suitable source for artificial conversion into different hydrocarbon products.
41	Khozyem et al. (2021)	Lignites from Panandhro mine, Bhavnagar mine, Vastan mine, Tadkeshwar mine & Giral mine, western India.	rock-eval pyrolysis, organic carbon isotope, biostratigraphy	*(i)* Identical deposition of lignites recorded for NW India, except for lignite intervals recorded in the Giral mine. A predominant terrestrial input for the deposition of lignites. *(ii)* A clear carbon isotopic excursion was found for Paleocene-Eocene Thermal Maximum (PETM) and Eocene Thermal Maximum 2 (ETM2) periods. *(iii)* The "into India" concept is supported by the relative location of the lignite mammal-bearing interval.
42	Kumar et al. (2021)	Matasukh, Gurha, Barsingsar mines, Bikaner-Nagaur basin, Rajasthan basin, western India.	Proximate & ultimate analysis, rock-eval pyrolysis, stable carbon isotope analysis, biomarker	*(i)* Groundwater level fluctuations reported from the variation in ash yield among the lignites. *(ii)* A marginal marine/brackish water habitat with an overall acidic state was prevalent. *(iii)* An OM input was predominantly from coastal or terrestrial vegetation mostly from ligno-cellulosic plants in addition to C3 plants and mangroves. A diagenetic stage thermal maturity reported for the OM. *(iv)* A change in palaeovegetation has been documented as a result of climatic fluctuations between humid and dry spells.
43	Kumar et al. (2021)	Paleogene lignites, Rajasthan, India	Lithotypes, petrography, proximate, ultimate, TOC, major oxides, ^{13}C NMR, and $\delta^{13}C$	*(i)* The Giral lignites show a rank B and are mostly immature. *(ii)* A dominant C3 plant input, both from gymnosperms and angiosperms, marked for the peak formation. *(iii)* A gently oxic to anoxic depositional environment with increased microbial activity marked the deposition of OM whereas peat developed mostly in a semi-arid to arid climate. *(iv)* Maceral study reveals some sort of marine incursion in to the basin.
44	Rajak et al. (2021)	Kapurdi lignites, Barmer Basin, Rajasthan, western India	Petrographic analysis, proximate & ultimate analysis, rock-eval pyrolysis, FTIR	*(i)* Kapurdi lignites are examined to be low-rank-C coals, with an OM input mostly from Type-III kerogen. *(ii)* The lignites have a high volatile matter and low-medium ash content. *(iii)* These are suitable candidates for source rock for producing hydrocarbon through artificial techniques. *(iv)* The high concentration of reactive macerals and low maturity of these lignites result in excellent conversion rates and high oil yield.
45	Choudhury et al. (2022)	Paleogene galuconites, western India. Kutch basin, Cambay basin, Jaisalmer basin, Barmer basin	Biostratigraphy, carbon isotope stratigraphy, petrography, mineral chemistry & major oxide concentration using EPMA	*(i)* Authigenic glauconites, with brief intervals of glauconitization, are common in the shallow marine Paleogene sedimentary basins of western India. *(ii)* The glauconites range in maturity from K-poor embryonic glauconite pellet in the Barmer Basin to fully developed glauconite pellet in the Jaisalmer Basin. Glauconite occurs shortly before the commencement of the PETM in the Jaisalmer Basin, whereas it appears just after the PETM in the nearby Barmer Basin. *(iii)* Despite their low maturity, the Glauconites are rich in Fe_2O_3. The kaolinite-rich clay substrate are responsible for the high Al_2O_3 composition of these glauconite pellets. *(iv)* Warming events during Early Paleogene are related to marine transgression, that supported glauconitization. However, PETM hindered glauconite formation.
46	Kar et al. (2022)	Giral lignite mine & Sarnoo siltstones, Barmer basin, western Rajasthan, India	Bulk OM analysis using rock-eval pyrolysis, kerogen kinetics using OPTKIN software	*(i)* Dominant heterogeneous Type-III kerogen input for Giral lignites. *(ii)* An excellent TOC of lignites and shaly lignites suggests better preservation of OM under a reducing environment. *(iii)* Organically lean nature of shales, is associated with a higher subsidence rate than peat accumulation. *(iv)* The Giral mine samples are excellent for artificial conversion into different hydrocarbon products.

Repository Table 1 continued…

Sl. No.	Author(s)	Mine	Techniques	Key conclusions
47	Kumar et al. (2022)	Kapurdi carbonaceous shales, Barmer Basin, Rajasthan, India	Petrography, pyrolysis-gas chromatography, TOC analysis, rock-eval pyrolysis, huminite reflectance	*(i)* The OM for the Kapurdi region is dominated by Type II-III kerogen and is mostly immature to early mature field. *(ii)* The shales are examined to be a good source rock for the generation of hydrocarbon with a potential to generate both oil and gas (mostly oil). *(iii)* The deeper stratigraphic extensions are suggested to have better maturity for petroleum production and exploration.
48	Singh et al. (2022)	Sonari lignite mine, Barmer Basin, Rajasthan, India	Petrography, palynofacies study, biomarker, rock-eval pyrolysis, proximate & ultimate analysis, gross calorific value analyses	*(i)* The Sonari lignites are rich in huminite group of macerals with OM contribution mostly from angiosperm and minor gymnosperm sources. *(ii)* The OM input is mostly from Type-III kerogen and mostly immature. Both terrestrial and marine signature for OM input recorded. The OM is suitable for artificial conversion upon maturation. *(iii)* The OM deposited in a limno-telmatic environment with shifting in groundwater level from mesotrophic to rheotrophic. A dysoxic-anoxic environment recorded intermediate suboxic condition. *(iv)* A coastal depositional setting such as back-barrier type environment proposed for the area.
49	Bhandari and Choudary (2023)	Kapurdi and Jalipa lignite mine	Enrichment and isolation of sulfur oxidising bacteria	*(i)* Lignite deposits in the Kapurdi and Jalipa mine host a lineage of sulfur-oxidizing bacteria. *(ii)* These bacteria have the potential to be used for lignite bio-desulfurization and bioleaching of heavy metals.
50	Kumar et al. (2023)	Giral, Sonari and Kapurdi mine, Barmer Basin, Rajasthan	XRD, XRF, Inductively coupled plasma mass spectrometry (ICPMS)	*(i)* Hematite, nepheline and anhydrite are the dominant minerals. *(ii)* Marine-influenced depositional setting marked from the presence of pyrite. *(iii)* These lignites possess good potential of Rare Earth Elements (REE).
51	Ganguly et al. (2023)	Umarsar, Matanomadh, Panandhro, Tadkeshwar lignite mine, Gujarat	Stable nitrogen isotope	*(i)* Lignites are rich in huminite followed by liptinite and intertinite. (ii) A moderate to strong correlation marked between C/N and δ15N in lignites from the Cambay Basin (R^2 = 0.49) and Kutch Basin (R^2 = 0.82) in Gujarat indicates a close link between nitrogen loss/incorporation and δ15N variation.
52	Ojha and Singh (2023)	Tharad Formation coals, Cambay Basin, Gujarat	Petrography, fluorescence microscopy, rock-eval pyrolysis, biomarker	*(i)* The coals are found to be of non-banded variety and rich in vitrinite macerals. The OM sourced from terrestrial forest plants that developed in a humid tropical conditions. *(ii)* Episodic marine incursion activity to the basin recorded. *(iii)* A fluvio-deltaic depositional environment recorded with support signature of tidal activities.
53	Shukla et al. (2023)	Gurha lignite mine, Bikaner basin, Rajasthan, India	Palynological analysis, petrography, SEM imagery, biomarker analysis	*(i)* The Gurha lignites are rich in huminite and inertinite groups of macerals. The OM input to the area is supposed to be from higher plants (both gymnosperms and angiosperms) and from herbaceous plants. *(ii)* A wildfire activity reported at the depositional setting with a burning temperature between 300-7980C. *(iii)* The early Paleogene monsoonal climate (wet/dry season) could be the reason for the ignition and for the spread of wildfires.
54	Kumar et al. (2024)	Giral and Kapurdi mine, Western Rajasthan, India	Huminite reflectance, Proximate and ultimate analysis, rock-eval pyrolysis, XRD, XRF	*(i)* A presence of telmatic condition lead to the accumulation of thick peat layers for both the mine. *(ii)* During peat accumulation, the paleoclimate was warm and humid, with rheotrophic conditions prevailing in the Giral paleomire due to sporadic lowering of the groundwater table, while in the Kapurdi paleomire, conditions were primarily ombrotrophic, with atmospheric precipitation exclusively supplying water. *(iii)* Barmer ortholignites are immature, but possess good potential for hydrocarbon generation.
55	Kumar et al. (2024)	Kapurdi, Giral, Sonari mine, Western Rajasthan, India	Proximate and ultimate analysis, FTIR, rock-eval pyrolysis,	*(i)* The coals are of low rank with high moisture and volatile matter. *(ii)* Lignites are dominated with huminite macerals followed by liptinite and intertinite. *(iii)* Type II-III kerogen with immature nature.
56	Kar et al. (2025, this work)	Giral lignite mine, western Rajasthan, India	Biomarker and carbon isotope analysis	*(i)* Giral mine lignites were deposited in an oxic to dysoxic environment, whereas the shaly lignite and shales deposited in an anoxic sulphidic environment. *(ii)* The OM input for the deposition of lignites is mainly incorporated from the terrestrial environment, while a marine lacustrine/estuarine input is marked for shaly lignite and shales. *(iii)* It is hypothesised that lithotype deposition may be impacted by periodic fluctuations in sea level in coastal habitats, notably those of the continental shelf type.

Repository Table 2. Correlation of important biomarker ratios with the global average value.

Ratios	Global average	Lignite	Shaly lignite	Shale	Reference
CPI	~ 1: thermally mature Significantly below or above 1: immature	0.84	0.74	0.7	Bray and Evans (1961); Peters et al., (2005b)
CPI1	5-10: vascular plants < 5: aquatic submergent plants and emergent vegetation & microbial action	3.87	2.92	2.11	Bechtel et al., (2001) Commendatore et al., (2012); Kanzari et al., (2014); El Nemr et al., (2016); Kumar et al., (2021)
CPI2	~ 1 or 1: Petroleum source < 1: Microbial activity	0.16	0.07	0.07	Clark and Blumer (1967); Garg and Bhosle (2004); Ahad et al., (2011); Pu-nyu et al., (2013); Kumar et al., (2021)
OEP1	< 1: even-over-odd preference (OM from aquatic vegetation and microbial activity) > 1: odd-over-even preference (Terrestrial input)	0.99	0.53	0.44	Scalan and Smith (1970); Kumar et al., (2021)
OEP2	> 1: waxy terrestrial OM, less biodegradation < 1: aquatic plants, more biodegradation	1.54	1.16	0.81	Scalan and Smith (1970); Kumar et al., (2021)
P_{aq}	< 0.1: Terrestrial plant 0.1-0.4: Emergent macrophyte 0.4-1: Submerged/floating macrophyte	0.21	0.3	0.41	Ficken et al., (2000)
TAR	> 1: lipid from watershed < 1: lipid from aquatic source (higher value terrestrial input, lower marks aquatic input)	12.9	6.09	3.04	Bourbonniere and Meyers (1996)
TMD	> 1: Terrestrial input 0.5-1: mixed source < 0.5: Marine/aquatic input (higher value terrestrial input, lower marks aquatic input)	6.96	4.93	2.93	Raja Chairi (2018)
Pr/Ph	< 2: marine/brackish water (reducing condition) 2-4: fluvio-marine and coastal swamp (oxic to suboxic) ~ 10: peat swamp (oxic environment)	6.81	0.91	0.76	Powell (1984); Lijmbach (1975)
LMWH/ HMWH	< 1: Terrestrial input > 1: aquatic/marine input	0.58	1.70	2.59	Gearing et al., (1976); Wang et al., (2006); Kanzaari et al., (2012)
Ts/(Ts+Tm)	< 1: immature ~ 1 or =1: mature	0.53	0.77	0.78	Hong et al., (1986); Peters et al., (2005b)
C$_{31}$ 22S/ (22S+22R)	~ 0-0.5: immature ~ 0.5-0.54: early oil window ~ 0.57-0.62: peak oil window	0.22	0.13	0.14	Seifert and Moldowan, (1978); Peters et al., (2005b)
%C_{27} Steranes	$(C_{27}+C_{28}) > C_{29}$: algal source $(C_{28}+C_{29}) > C_{27}$: mixed source $(C_{27}+C_{28}) < C_{29}$: terrestrial source	12.26	55.76	43.79	Lijmbach (1975); Peters et al., (2005b)
%C_{28} Steranes		48.73	15.9	16.44	
%C_{29} Steranes		39.01	28.33	39.77	

Repository Table 3. Remaining organic geochemical work for Gujarat and Rajasthan Basin, western India. * = Remaining work, ** = Biomarker work done for resins, not for lignites/shales, ***= work presented in this study.

Mine	Petrography	Proximate analysis	Ultimate analysis	Rock-Eval pyrolysis	Kerogen Kinetics	Biomarker analysis	Huminite reflectance	Carbon isotope
Giral, Rajasthan						***		***
Kapurdi, Rajasthan					*			*
Sonari, Rajasthan					*			
Gurha					*			*
Barsingsar					*			
Matasukh					*			
Umarsar					*	*		
Vastan					*	**		
Panandhro		*			*	**		
Bhavnagar					*	*		
Surkha					*			*

Repository Table 3 continued…

Mine	Petrography	Proximate analysis	Ultimate analysis	Rock-Eval pyrolysis	Kerogen Kinetics	Biomarker analysis	Huminite reflectance	Carbon isotope
Rajpardi					*	*		*
Tadkeshwar					*	**		
Matanomadh		*			*	*		

Calculations related to Table 3 in the main text:

Carbon preference Index (CPI) following Bray and Evans (1961):

$CPI=\{[(C_{25}+C_{27}+C_{29}+C_{31}+C_{33})/(C_{24}+C_{26}+C_{28}+C_{30}+C_{32})]+[(C_{25}+C_{27}+C_{29}+C31+C_{33})/(C_{26}+C_{28}+C_{30}+C_{32}+C_{34})]\}/2$

Carbon preference index1 (CPI1) after El-Nemr *et al.* (2016):

$CPI1= [(C_{23}+C_{25}+C_{27}+C_{29}+C_{31})+(C_{25}+C_{27}+C_{29}+C_{31}+C_{33})]/2*(C_{24}+C_{26}+C_{28}+C_{30}+C_{32})$

Carbon preference index2 (CPI2) after Punyu *et al.* (2013):

$CPI2= (C_{11}+C_{13}+C_{15}+C_{17}+C_{19}+C_{21})/(C_{12}+C_{14}+C_{16}+C_{18}+C_{20})$

Odd to even preference1 (OEP1) after Scalan and Smith (1970) and Peters *et al.* (2005b):

$OEP1= [C_{21}+(6*C_{23})+C_{25}]/4*(C_{22}+C_{24})$

Odd to even preference2 (OEP2) after Scalan and Smith (1970) and Peters et al., (2005b):

$OEP2= [C_{25}+(6*C_{27})+C_{29}]/(4*(C_{26}+C_{28})$

Proxy-aqueous ratio (P_{aq}) after Ficken *et al.* (2000):

$P_{aq} = (C_{23}+C_{25})/(C_{23}+C_{25}+C_{29}+C_{31})$

Terrestrial aquatic ratio (TAR) after Bourbonniere and Meyers (1996):

$TAR= (C_{27}+C_{29}+C_{31})/(C_{15}+C_{17}+C_{19})$

Terrestrial marine discriminant ratio (TMD) after Raja Chairi (2018):

$TMD= (C_{25}+C_{27}+C_{29}+C_{31}+C_{33})/(C_{15}+C_{17}+C_{19}+C_{21}+C_{23})$

The ratio of low molecular weight hydrocarbon to high molecular weight hydrocarbon (LMWH/HMWH) after Gearing *et al.* (1976) and Wang *et al.* (2006):

$LMWH/HMWH= (C_{14}+C_{15}+C_{16}+C_{17}+C_{18}+C_{19}+C_{20})/(C_{21}+C_{22}+C_{23}+C_{24}+C_{25}+C_{26}+C_{27}+C_{28}+C_{29}+C_{30}+C_{31}+C_{32}+C_{33}+C_{34})$

Sample processing in the lab

Samples were cleansed in Milli-Q water, air-dried, then pulverized into a fine powder with an agate mortar. The bitumen fraction was extracted from the homogeneously pulverized samples for biomarker studies. Additionally, these samples were used to isolate kerogen for carbon isotope studies. Biomarkers were analyzed using the gas chromatography mass spectrometry (GC-MS) instrument at the Analytical and Structural Chemistry Department, CSIR-Indian Institute of Chemical Technology. Carbon Isotopes were analyzed using the MAT-253 elemental analyser isotope ratio mass spectrometer (MAT-253 EA-IRMS) instrument at the Department of Earth Sciences, Indian Institute of Technology Roorkee.

Solvent extraction

A Soxhlet extraction apparatus was used to extract organic matter (EOM) from the samples. The equipment includes an extractor, a condenser, a collector and a heating mantle. In a 100 ml extractor, 4 g of powdered sample was placed in a glass fibre thimble. 4 μl of the recovery standard *n*-hexatriacontane-d74 (*n*-C_{36}D74) was added to the sample. In the collector, about 120-130 ml DCM: MeOH (9:1) solvent mixture was taken and placed over the heating mantle. The components were then correctly assembled, the heating mantle temperature was set to the boiling point of the solvent (about 40 °C); and cold water was circulated to the condenser. The solvent in the collector was brought to a boil by the heating mantle. The vapour, condensed by the condenser, fell as droplets onto the sample in the extractor and the soluble bitumen portion of the sample leached out into the solvent. The entire solvent, mixed with the sample, was emptied into the collector via syphoning after the extractor reached its maximum capacity, thus completing one extraction cycle. Until all of the bitumen from the powdered rocks were extracted, the process was resumed for up to 18 hours with nearly 60-70 cycles of Soxhlet extraction.

The EOM was concentrated in a rotary evaporator to ~ 6-8 ml. Later, employing a moderate nitrogen flow, the (EOM) was concentrated to a volume of ~ 1 ml mg^{-1} of EOM. It was then dissolved in 3 μl of DCM: MeOH (93:7 v/v) to remove the asphaltene fraction, and *n*-pentane was added to a 40-fold excess volume of EOM+DCM: MeOH. Sulfur was subsequently removed from the resulting maltene fraction using activated copper. This solvent extraction process was followed as per Anabtawi (1996).

Column chromatography

Silica gel column chromatography was used to separate the aliphatic, aromatic and polar fractions. 10 cm of silica gel 60 (70-230 mesh) was placed within a 30*2 cm^2 id burette. The silica column's top was loaded with the EOM mixture. *n*-Hexane was used to elute the aliphatic fraction, *n*-Hexane:DCM (1:4) was utilized to elute the aromatic portion, and DCM: MeOH was applied to elute the polar fraction (1:1). The solvent fractions were dried entirely under a gentle stream of N_2 gas to determine the recovery weight of all the extracted fractions (Bastow et al., 2007).

Gas chromatography-mass spectrometry (GC-MS)

Thermo Scientific Trace 1300 Gas Chromatography (GC) equipped with a TG-5MS (30 m * 0.25 mm * 0.25 µm) column coupled with a TSQ 9000 Triple Quadrupole Gas Chromatography-Mass Spectrometer (GC-MS) system was used to analyse the isolated aliphatic fractions. The temperature of the injector port was maintained at 300 °C. The GC oven's temperature was adjusted to 40 °C for a minute, then 140 °C at a rate 8 °C per minute, and then 290 °C at 5 °C per 1 minute. A carrier gas He was used with 99.999% purity at 1.2 ml min-1 flow rate. The data acquisition method was in electron ionisation (EI) mode at 70 eV. Ion source and MS transfer line temperatures were set at 240 °C and 290 °C, respectively. The filament emissions current was set at 50 A with a solvent delay of 6 min. The auto sampler was used to inject 2 µL of the analyte into the GC-MS in splitless mode. The mass range (*m/z*) of the GC-MS, which was in full scan mode, was 40-600 amu. The *n*-alkanes, isoprenoids, hopanes (Table 1 in the main text) and steranes (Table 2 in the main text) were identified using chromatograms with *m/z* values of 57, 183, 191 and 217, respectively. The current National Institutes of Standards and Technology (NIST) library and chromatograms of JR-1 and SR-1 standards obtained using the above protocols were used to match the GC retention durations, fragmentation patterns and *m/z* peaks of the ions (Philp & Gilbert 1985).

Kerogen separation & carbon isotope analysis

The kerogen content of the lignite, shaly lignite and shale samples was isolated following the procedure of Sekine *et al.* (2010). About 1 g sample was treated to 4N HCl in order to remove the inorganic carbon component. It was washed thrice with MQ water to get rid of the salts. The kerogen fractions were dried in an oven at 100 °C. The samples were further crushed uniformly and packed in Tin foils in accordance with their TOC for carbon isotope analysis.

Stable carbon isotope was analysed using the MAT-253 EA-IRMS equipment. For both the sample and the reference gas, signal equivalent to masses 44, 45 and 46 were detected, and the isotopic composition was computed. In order to verify the precision of the CO_2 readings, soil standards were used. The isotope values were then compared to Vienna Pee Dee Belemnite (V-PDB) and reported in per-mil (‰) units.

Abbreviations used in the main text:

CPI	Carbon preference index
DCM	Dichloromethane
DDF	Dharvi Dungar Formation
EA-IRMS	Elemental analyser isotope ratio mass spectrometer
EOM	Extracted organic matter
EOP	Even-to-odd predominance
ETM	Eocene thermal maximum
FTIR	Fourier-transform infrared
GC	Gas chromatography
GC-MS	Gas chromatography mass spectrometer
HC	Hydrocarbon
HMWH	High molecular weight hydrocarbon
LMWH	Low molecular weight hydrocarbon
MeOH	Methanol
NIST	National institute of standards and technology
OEP	Odd-to-Even preference
OM	Organic matter
P_{aq}	Proxy ratio
PETM	Paleocene Eocene thermal maximam
Ph	Phytane
Pr	Pristane
REE	Rare earth elements
SEM	Scanning electron microscopy
SEM-EDS	Scanning electron microscopy and energy-dispersive X-ray spectroscopy
TAR	Terrestrial aquatic ratio
Tm	17α-22,29,30-trisnorhopane
T_{max}	Temperature at which maximum amount of hydrocarbon gets released by the cracking of kerogen
TMD	Terrestrial marine discriminant
TOC	Total organic carbon
Ts	18α-22,29,30-trisnorhopane
TS	Total Sulfur
V-PDB	Vienna Pee Dee Belemnite
XRD	X-ray diffraction
XRF	X-ray fluorescence

REFERENCES

Ahad, J.M., Ganeshram, R.S., Bryant, C.L., Cisneros-Dozal, L.M., Ascough, P.L., Fallick, A. E. and Slater, G. F. (2011) Sources of n-alkanes in an urbanized estuary: Insights from molecular distributions and compound-specific stable and radiocarbon isotopes. *Marine Chemistry*, 126(1-4), 239-249. DOI: https://doi.org/10.1016/j.marchem.2011.06.002

Anabtawi, M.Z. (1996) Comparison between continuous stirred tank reactor extractor and soxhlet extractor for extraction of El-Lajjun oil shale. *Separation science and technology*, 31(3), 413-422. DOI: https://doi.org/10.1080/01496399608000704

Bastow, T.P., van Aarssen, B.G. and Lang, D. (2007) Rapid small-scale separation of saturate, aromatic and polar components in petroleum. *Organic Geochemistry*. 38(8), 1235-1250. DOI: https://doi.org/10.1016/j.orggeochem.2007.03.004

Bechtel, A., Gruber, W., Sachsenhofer, R.F., Gratzer, R. and Püttmann, W. (2001) Organic geochemical and stable carbon isotopic investigation of coals formed in low-lying and raised mires within the Eastern Alps (Austria). *Organic Geochemistry. 32*(11), 1289-1310. DOI: https://doi.org/10.1016/S0146-6380(01)00101-2

Bhandari, P. and Choudhary, S. (2023) Geomicrobial exploration of sulfur oxidizing bacteria indigenous to Kapurdi and Jalipa lignite mine site, Rajasthan. *Journal of the Geological Society of India. 99*(11), 1586-1594. DOI: https://doi.org/10.1007/s12594-023-2510-y

Bourbonniere, R.A. and Meyers, P.A. (1996) Sedimentary geolipid records of historical changes in the watersheds and productivities of Lakes Ontario and Erie. *Limnology and Oceanography. 41*(2), 352-359. DOI: https://doi.org/10.4319/lo.1996.41.2.0352

Bray, E.E. and Evans, E.D. (1961) Distribution of n-paraffins as a clue to recognition of source beds. *Geochimica et Cosmochimica Acta. 22*(1), 2-15. DOI: https://doi.org/10.1016/0016-7037(61)90069-2

Chairi, R. (2018) Biomarkers on sediments in a highly saline aquatic ecosystem: case of the Moknine Continental Sebkha (Eastern Tunisia). *Journal of Coastal Zone Management. 21*(2). DOI: 10.4172/2473-3350.1000463

Choudhury, T.R., Khanolkar, S. and Banerjee, S. (2022) Glauconite authigenesis during the warm climatic events of Paleogene: Case studies from shallow marine sections of Western India. *Global and Planetary Change. 214*, 103857. DOI: https://doi.org/10.1016/j.gloplacha.2022.103857

Clark, Jr, R.C. and Blumer, M. (1967) Distribution of n-paraffins in marine organisms and sediment. *Limnology and Oceanography. 12*(1), 79-87. DOI: https://doi.org/10.4319/lo.1967.12.1.0079

Commendatore, M.G., Nievas, M.L., Amin, O. and Esteves, J.L. (2012) Sources and distribution of aliphatic and polyaromatic hydrocarbons in coastal sediments from the Ushuaia Bay (Tierra del Fuego, Patagonia, Argentina). *Marine Environmental Research. 74*, 20-31. DOI: https://doi.org/10.1016/j.marenvres.2011.11.010

Das, S.K., Ganguly, M., Ghosh, M., Mani, D., Kalpana, M.S. and Kumar, S. (2021) Role of tectonic activities on kerogen maturity and carbon stable isotope signature of coal. *Journal of Earth System Science. 130*, 1-16. DOI: https://doi.org/10.1007/s12040-021-01707-x

Dutta, S., Mallick, M., Bertram, N., Greenwood, P.F. and Mathews, R.P. (2009) Terpenoid composition and class of Tertiary resins from India. *International Journal of Coal Geology. 80*(1), 44-50. DOI: https://doi.org/10.1016/j.coal.2009.07.006

Dutta, S., Mathews, R.P., Singh, B.D., Tripathi, S.M., Singh, A., Saraswati, P.K. and Mann, U. (2011) Petrology, palynology and organic geochemistry of Eocene lignite of Matanomadh, Kutch Basin, western India: Implications to depositional environment and hydrocarbon source potential. *International Journal of Coal Geology. 85*(1), 91-102. DOI: https://doi.org/10.1016/j.coal.2010.10.003

El Nemr, A., Moneer, A.A., Ragab, S. and El Sikaily, A. (2016) Distribution and sources of n-alkanes and polycyclic aromatic hydrocarbons in shellfish of the Egyptian Red Sea coast. *Egyptian Journal of Aquatic Research. 42*(2), 121-131. DOI: https://doi.org/10.1016/j.ejar.2016.05.003

Ficken, K.J., Li, B., Swain, D.L. and Eglinton, G. (2000) An n-alkane proxy for the sedimentary input of submerged/floating freshwater aquatic macrophytes. *Organic Geochemistry. 31*(7-8), 745-749. DOI: https://doi.org/10.1016/S0146-6380(00)00081-4

Ganguly, M., Das, S.K., Ekblad, A. and Behera, P.K. (2023) Variation of δ15N in Indian coal, lignite and peat. *Geochemistry. 83*(4), 126013. DOI: https://doi.org/10.1016/j.chemer.2023.126013

Garg, A. and Bhosle, N. (2004) Abundance of macroalgal organic matter in biofilms: evidence from n-alkane biomarkers. *Biofouling. 20*(3), 155-165. DOI: https://doi.org/10.1080/08927010400001816

Gearing, P., Gearing, J.N., Lytle, T.F. and Lytle, J.S. (1976) Hydrocarbons in 60 northeast Gulf of Mexico shelf sediments: a preliminary survey. *Geochimica et Cosmochimica Acta. 40*(9), 1005-1017. DOI: https://doi.org/10.1016/0016-7037(76)90043-0

Hakimi, M.H., Kumar, A., Singh, A.K., Lashin, A., Rahim, A., Varfolomeev, M.A. and Mustapha, K.A. (2023) Geochemistry and organic petrology of the bituminite shales from the Kapurdi mine, Rajasthan of NW India: implications for waxy oil generation potential. *Journal of Petroleum Exploration and Production Technology. 13*(2), 505-521. DOI: https://doi.org/10.1007/s13202-022-01597-9

Zhi-Hua, H., Hui-Xiang, L., Rullkötter, J. and Mackenzie, A.S. (1986) Geochemical application of sterane and triterpane biological marker compounds in the Linyi Basin. *Organic Geochemistry. 10*(1-3), 433-439. DOI: https://doi.org/10.1016/0146-6380(86)90043-4

Kanzari, F., Syakti, A.D., Asia, L., Malleret, L., Piram, A., Mille, G. and Doumenq, P. (2014) Distributions and sources of persistent organic pollutants (aliphatic hydrocarbons, PAHs, PCBs and pesticides) in surface sediments of an industrialized urban river (Huveaune), France. *Science of the Total Environment. 478*, 141-151. DOI: https://doi.org/10.1016/j.scitotenv.2014.01.065

Kar, N.R., Mani, D., Mukherjee, S., Dasgupta, S., Puniya, M.K., Kaushik, A.K. and Babu, E.V.S.S.K. (2022) Source rock properties and kerogen decomposition kinetics of Eocene shales from petroliferous Barmer basin, western Rajasthan, India. *Journal of Natural Gas Science and Engineering. 100*, 104497. DOI: https://doi.org/10.1016/j.jngse.2022.104497

Kar, N.R., Mani, D., Seetha, B.S., Babu, E.V.S.S.K., Mukherjee, S., Dasgupta, S. and Mudiam, M.K.R. (2025, this work) Biomarker evidence of shifts in organic provenance and depositional environments of Eocene carbonaceous rocks from petroliferous Barmer basin, western Rajasthan, India. *Journal of the Geological Society of India.*

Khozyem, H., Adatte, T., Keller, G. and Spangenberg, J.E. (2021) Organic carbon isotope records of the Paleocene-Eocene thermal maximum event in India provide new insights into mammal origination and migration. *Journal of Asian Earth Sciences. 212*, 104736. DOI: https://doi.org/10.1016/j.jseaes.2021.104736

Kumar, A., Hakimi, M.H., Singh, A.K., Abdullah, W.H., Zainal Abidin, N.S., Rahim, A. and Yelwa, N.A. (2022) Geochemical and petrological characterization of the early Eocene carbonaceous shales: Implications for oil and gas exploration in the Barmer Basin, Northwest India. *ACS Omega. 7*(47), 42960-42974. DOI: https://doi.org/10.1021/acsomega.2c05148

Kumar, A., Singh, A.K. and Christanis, K. (2024) Paleodepositional environment and hydrocarbon generation potential of the Paleogene lignite in the Barmer Basin, Rajasthan, India. *Journal of Asian Earth Sciences. 259*, 105892. DOI: https://doi.org/10.1016/j.jseaes.2023.105892

Kumar, A., Singh, A.K., Paul, D. and Kumar, A. (2020) Evaluation of hydrocarbon potential with insight into climate and environment present during deposition of the Sonari lignite, Barmer Basin Rajasthan. *Energy and Climate Change. 1*, 100006. DOI: https://doi.org/10.1016/j.egycc.2020.100006

Kumar, A., Singh, A.K., Singh, P.K., Singh, A.L., Saikia, B.K. and Kumar, A. (2022) Desulfurization of giral lignite of Rajasthan (Western India) using Burkholderia sp. GR 8–02. *International Journal of Coal Preparation and Utilization. 42*(3), 735-751. DOI: https://doi.org/10.1080/19392699.2019.1651721

Kumar, A., Singh, A.K., Paul, D. and Kumar, A. (2021) Paleoenvironmental, paleovegetational, and paleoclimatic changes during Paleogene lignite formation in Rajasthan, India. *Arabian Journal of Geosciences. 14*, 1-15. DOI: https://doi.org/10.1007/s12517-021-08638-3

Kumar, D., Ghosh, S., Tiwari, B., Varma, A.K., Mathews, R.P. and Chetia, R. (2021) Palaeocene-Eocene organic sedimentary archives of Bikaner-Nagaur Basin, Rajasthan, India: An integrated revelation from biogeochemical and elemental proxies. *International Journal of Coal Geology. 247*, 103848. DOI: https://doi.org/10.1016/j.coal.2021.103848

Kumar, O.P., Gopinathan, P., Naik, A.S., Subramani, T., Singh, P.K., Sharma, A. and Saha, S. (2023) Characterization of lignite deposits of Barmer Basin, Rajasthan: insights from mineralogical and elemental analysis. *Environmental Geochemistry and Health. 45*(8), 6471-6493. DOI: https://doi.org/10.1007/s10653-023-01649-x

Kumar, O.P., Naik, A.S., Gopinathan, P., Subramani, T., Singh, V., Singh, P.K. and Prabhu, A. (2024) Petrographic and geochemical analysis of Barmer Basin Paleogene lignite deposits: Insights into depositional environment and paleo-climate. *Journal of Geochemical Exploration. 256*, 107335. DOI: https://doi.org/10.1016/j.gexplo.2023.107335

Kumar, S., Ojha, K., Bastia, R., Garg, K., Das, S. and Mohanty, D. (2017) Evaluation of Eocene source rock for potential shale oil and gas generation in north Cambay Basin, India. *Marine and Petroleum Geology. 88*, 141-154. DOI: https://doi.org/10.1016/j.marpetgeo.2017.08.015

Kumar, S., Singh, A. and Dogra, N.N. (2013) Huminite Reflectance Attributes for Rank Estimation of Panandhro Lignite Deposit (Kutch Basin), Gujarat, India. *Gondwana Geol. Mag. 28*, 11-16.

Lijmbach, G. (1975) On the origin of petroleum: proceedings of the 9th world petroleum congress. *Applied Science Publishers.* London, 2, 357-369.

Mallick, M., Dutta, S., Greenwood, P.F. and Bertram, N. (2009) Pyrolytic and spectroscopic studies of Eocene resin from Vastan lignite mine, Cambay Basin, western India. *Journal of the Geological Society of India. 74*, 16-22. DOI: https://doi.org/10.1007/s12594-009-0098-5

Mathews, R.P., Chetia, R., Agrawal, S., Singh, B.D., Singh, P.K., Singh, V.P. and Singh, A. (2020) Early Palaeogene climate variability based on n-alkane and stable carbon isotopic composition evidenced from the Barsingsar Lignite-bearing sequence of Rajasthan. *Journal of the Geological Society of India. 95*, 255-262. DOI: https://doi.org/10.1007/s12594-020-1423-2

Mathews, R.P., Singh, B.D., Singh, H., Singh, V.P. and Singh, A. (2018) Characterization of Panandhro Lignite deposits (Kachchh Basin), western India: Results from the bulk geochemical and palynofloral compositions. *Journal of the Geological Society of India. 91*(3), 281-289. DOI: https://doi.org/10.1007/s12594-018-0851-8

Mathews, R.P., Singh, B.D., Singh, V.P., Singh, A., Singh, H., Shivanna, M. and Chetia, R. (2020) Organo-petrographic and geochemical characteristics of Gurha lignite deposits, Rajasthan, India: Insights into the palaeovegetation, palaeoenvironment and hydrocarbon source rock potential. *Geoscience Frontiers. 11*(3), 965-988. DOI: https://doi.org/10.1016/j.gsf.2019.10.002

Mishra, S., Mani, D., Kavitha, S., Kalpana, M.S., Patil, D.J., Vyas, D.U. and Dayal, A.M. (2014) Organic matter characteristics and gas generation potential of the Tertiary shales from NW Kutch, India. *Journal of Petroleum Science and Engineering, 124*, 114-121. DOI: https://doi.org/10.1016/j.petrol.2014.10.019

Mukherjee, A.K., Alam, M.M., Mazumdar, S.K., Haque, R. and Gowrisankaran, S. (1992) Physico-chemical properties and petrographic characteristics of the Kapurdi lignite deposit, Barmer Basin, Rajasthan, India. *International Journal of Coal Geology, 21*(1-2), 31-44. DOI: https://doi.org/10.1016/0166-5162(92)90034-T

Ojha, S. and Singh, P.K. (2023) Petrogenesis and Evolution of Tharad Coals of Cambay Basin, Gujarat (Western India): An Insight. *Journal of the Geological Society of India, 99*(5), 675-687. DOI: https://doi.org/10.1007/s12594-023-2368-z

Paul, S. and Dutta, S. (2016) Terpenoid composition of fossil resins from western India: New insights into the occurrence of resin-producing trees in Early Paleogene equatorial rainforest of Asia. *International Journal of Coal Geology, 167*, 65-74. DOI: https://doi.org/10.1016/j.coal.2016.09.008

Paul, S., Sharma, J., Singh, B. D., Saraswati, P. K. and Dutta, S. (2015) Early Eocene equatorial vegetation and depositional environment: Biomarker and palynological evidences from a lignite-bearing sequence of Cambay Basin, western India. *International Journal of Coal Geology, 149*, 77-92. DOI: https://doi.org/10.1016/j.coal.2015.06.017

Peters, K. E., Walters, C. C. and Moldowan, J. M. (2005b) The Biomarker Guide, Volume 2: Biomarkers and Isotopes in the Petroleum Exploration and Earth History; Cambridge University Press, Cambridge, UK.

Philp, R. P. and Gilbert, T. D. (1985) Source rock and asphaltene biomarker characterization by pyrolysis-gas chromatography-mass spectrometry-multiple ion detection. *Geochimica et Cosmochimica Acta, 49*(6), 1421-1432. DOI: https://doi.org/10.1016/0016-7037(85)90292-3

Powell, T. G. (1984) Developments in concept of hydrocarbon generation from terrestrial organic matter. Beijing Petroleum Symposium (20-24 Sept. 1984), Beijing, China.

Prasad, V., Uddandam, P.R., Agrawal, S., Bajpai, S., Singh, I., Mishra, A.K. and Verma, P. (2020) Biostratigraphy, palaeoenvironment and sea level changes during pre-collisional (Palaeocene) phase of the Indian plate: palynological evidence from Akli Formation in Giral Lignite Mine, Barmer Basin, Rajasthan, Western India. *Episodes Journal of International Geoscience. 43*(1), 476-488. DOI: https://doi.org/10.18814/epiiugs/2020/020030

Punyu, V.R., Harji, R.R., Bhosle, N.B., Sawant, S.S. and Venkat, K. (2013) n-Alkanes in surficial sediments of Visakhapatnam harbour, east coast of India. *Journal of Earth System Science. 122*(2), 467-477. DOI: https://doi.org/10.1007/s12040-013-0268-0

Rajak, P.K., Singh, V.K. and Singh, P.K. (2019) Distribution of inertinites in the Early Paleogene lignites of Western India: on the possibility of wildfire activities. *Journal of the Geological Society of India. 93*, 523-532. DOI: https://doi.org/10.1007/s12594-019-1213-x

Rajak, P.K., Singh, V.K., Kumar, A., Singh, V., Rai, A., Rai, S. and Singh, P.K. (2021) Study of hydrocarbon source potential of Kapurdi lignites of Barmer basin, Rajasthan, western India. *Journal of the Geological Society of India. 97*, 836-842. DOI: https://doi.org/10.1007/s12594-021-1782-3

Rajak, P.K., Singh, V.K., Singh, A.L., Kumar, N., Kumar, O.P., Singh, V. and Singh, P.K. (2020) Study of minerals and selected environmentally sensitive elements in Kapurdi lignites of Barmer Basin, Rajasthan, western India: implications to environment. *Geosciences Journal. 24*, 441-458. DOI: https://doi.org/10.1007/s12303-019-0029-4

Rajak, P.K., Singh, V.K., Singh, P.K., Singh, A.L., Kumar, N., Kumar, O.P. and Kumar, A. (2018) Geochemical implications of minerals and environmentally sensitive elements of Giral lignite, Barmer Basin, Rajasthan (India). *Environmental Earth Sciences. 77*, 1-20. DOI: https://doi.org/10.1007/s12665-018-7885-5

Roy Choudhury, T., Banerjee, S., Khanolkar, S. and Meena, S.S. (2021) Paleoenvironmental conditions during the Paleocene–Eocene transition imprinted within the glauconitic Giral Member of the Barmer Basin, India. *Minerals. 12*(1), 56. DOI: https://doi.org/10.3390/min12010056

Scalan, E.S. and Smith, J.E. (1970) An improved measure of the odd-even predominance in the normal alkanes of sediment extracts and petroleum.

Geochimica et Cosmochimica Acta. 34(5), 611-620. DOI: https://doi.org/10.1016/0016-7037(70)90019-0

Seifert, W.K. and Moldowan, J.M. (1978) Applications of steranes, terpanes and monoaromatics to the maturation, migration and source of crude oils. *Geochimica et Cosmochimica Acta. 42*(1), 77-95. DOI: https://doi.org/10.1016/0016-7037(78)90219-3

Sekine, Y., Tajika, E., Ohkouchi, N., Ogawa, N.O., Goto, K., Tada, R., ... and Kirschvink, J.L. (2010) Anomalous negative excursion of carbon isotope in organic carbon after the last Paleoproterozoic glaciation in North America. *Geochemistry, Geophysics, Geosystems. 11*(8). DOI: https://doi.org/10.1029/2010GC003210

Shukla, A., Jasper, A., Uhl, D., Mathews, R.P., Singh, V.P., Chandra, K. and Mehrotra, R.C. (2023) Paleo-wildfire signatures revealing co-occurrence of angiosperm-gymnosperm in the early Paleogene: Evidences from woody charcoal and biomarker analysis from the Gurha lignite mine, Rajasthan, India. *International Journal of Coal Geology. 265*, 104164. DOI: https://doi.org/10.1016/j.coal.2022.104164

Singh, A.K. and Kumar, A. (2017) Petro-chemical characterisation and depositional paleoenvironment of lignite deposits of Nagaur, Western Rajasthan, India. *Environmental Earth Sciences. 76*, 1-18. DOI: https://doi.org/10.1007/s12665-017-7004-z

Singh, A.K. and Kumar, A. (2018) Organic geochemical characteristics of Nagaur lignites, Rajasthan, India, and their implication on thermal maturity and paleoenvironment. *Energy Sources, Part A: Recovery, Utilization, and Environmental Effects. 40*(15), 1842-1851. DOI: https://doi.org/10.1080/15567036.2018.1487480

Singh, A.K., Hakimi, M.H., Kumar, A., Ahmed, A., Abidin, N.S.Z., Kinawy, M. and Lashin, A. (2020) Geochemical and organic petrographic characteristics of high bituminous shales from Gurha mine in Rajasthan, NW India. *Scientific Reports. 10*(1), 22108. DOI: https://doi.org/10.1038/s41598-020-78906-x

Akanksha, Singh, A.K., Mohanty, D. and Jena, H.M. (2020) Prospective evaluation of hydrocarbon generation potential of Umarsar lignite, India. *Energy Sources, Part A: Recovery, Utilization, and Environmental Effects. 42*(6), 664-675. DOI: https://doi.org/10.1080/15567036.2019.1588430

Singh, A.K., Kumar, A., and Hakimi, M.H. (2018) Organic geochemical and petrographical characteristics of the Nagaur lignites, Western Rajasthan, India and their relevance to liquid hydrocarbon generation. *Arabian Journal of Geosciences. 11*, 1-15. DOI: https://doi.org/10.1007/s12517-018-3744-7

Singh, A.K., Kumar, A., Singh, P.K., Singh, A.L., and Kumar, A. (2018) Bacterial desulphurization of low-rank coal: A case study of Eocene Lignite of Western Rajasthan, India. *Energy Sources, Part A: Recovery, Utilization, and Environmental Effects. 40*(10), 1199-1208. DOI: https://doi.org/10.1080/15567036.2018.1476608

Singh, A., Shivanna, M., Mathews, R.P., Singh, B.D., Singh, H., Singh, V.P. and Dutta, S. (2017) Paleoenvironment of Eocene lignite bearing succession from Bikaner-Nagaur Basin, western India: organic petrography, palynology, palynofacies and geochemistry. *International Journal of Coal Geology. 181,* 87-102. DOI: https://doi.org/10.1016/j.coal.2017.08.009

Singh, P.K. (2012) Petrological and Geochemical considerations to predict oil potential of Rajpardi and Vastan lignite deposits of Gujarat, Western India. *Journal of the Geological Society of India. 80*, 759-770. DOI: https://doi.org/10.1007/s12594-012-0206-9

Singh, P.K., Rajak, P.K., Singh, M.P., Naik, A.S., Singh, V.K., Raju, S.V. and Ojha, S. (2015) Environmental Geochemistry of selected elements in lignite from Barsingsar and Gurha Mines of Rajasthan, Western India. *Journal of the Geological Society of India. 86*, 23-32. DOI: https://doi.org/10.1007/s12594-015-0277-5

Singh, P.K., Rajak, P.K., Singh, M.P., Singh, V.K., Naik, A.S. and Singh, A.K. (2016) Peat swamps at Giral lignite field of Barmer basin, Rajasthan, Western India: understanding the evolution through petrological modelling. *International Journal of Coal Science & Technology. 3*, 148-164. DOI: https://doi.org/10.1007/s40789-016-0137-y

Singh, P.K., Rajak, P.K., Singh, V.K., Singh, M.P., Naik, A.S. and Raju, S.V. (2016) Studies on thermal maturity and hydrocarbon potential of lignites of Bikaner–Nagaur basin, Rajasthan. *Energy Exploration & Exploitation. 34*(1), 140-157. DOI: https://doi.org/10.1177/0144598715623679

Singh, P.K., Singh, M.P. and Singh, A.K. (2010) Petro-chemical characterization and evolution of Vastan Lignite, Gujarat, India. *International Journal of Coal Geology. 82*(1-2), 1-16. DOI: https://doi.org/10.1016/j.coal.2010.01.003

Singh, P.K., Singh, M.P., Singh, A.K., Naik, A.S., Singh, V.K., Singh, V.K. and Rajak, P.K. (2012) Petrological and geochemical investigations of Rajpardi lignite deposit, Gujarat, India. *Energy Exploration & Exploitation. 30*(1), 131-151. DOI: https://doi.org/10.1260/0144-5987.30.1.131

Singh, P.K., Singh, V.K., Rajak, P.K., Singh, M.P., Naik, A.S., Raju, S.V. and Mohanty, D. (2016) Eocene lignites from Cambay basin, Western India: an excellent source of Hydrocarbon. *Geoscience Frontiers. 7*(5), 811-819. DOI: https://doi.org/10.1016/j.gsf.2015.08.001

Singh, P.K., Singh, V.K., Singh, M.P. and Rajak, P.K. (2017) Paleomires of eocene lignites of Bhavnagar, Saurashtra basin (Gujarat), western India: petrographic implications. *Journal of the Geological Society of India. 90*, 9-19. DOI: https://doi.org/10.1007/s12594-017-0658-z

Singh, A.K. and Kumar, A. (2020) Assessment of thermal maturity, source rock potential and paleodepositional environment of the Paleogene lignites in Barsingsar, Bikaner–Nagaur Basin, Western Rajasthan, India. *Natural Resources Research. 29*(2), 1283-1305. DOI: https://doi.org/10.1007/s11053-019-09502-8

Singh, V.K., Rajak, P.K. and Singh, P.K. (2019) Revisiting the paleomires of western India: An insight into the early Paleogene lignite Corridor. *Journal of Asian Earth Sciences. 171*, 363-375. DOI: https://doi.org/10.1016/j.jseaes.2018.08.031

Singh, V.P., Singh, B.D., Mathews, R.P., Singh, A., Mendhe, V.A., Mishra, S. and Banerjee, M. (2022) Paleodepositional and hydrocarbon source-rock characteristics of the Sonari succession (Paleocene), Barmer Basin, NW India: implications from petrography and geochemistry. *Natural Resources Research. 31*(5), 2943-2971. DOI: https://doi.org/10.1007/s11053-022-10079-y

Singh, V.P., Singh, B.D., Mathews, R.P., Singh, A., Mendhe, V.A., Singh, P.K. and Singh, M.P. (2017) Investigation on the lignite deposits of Surkha mine (Saurashtra Basin, Gujarat), western India: Their depositional history and hydrocarbon generation potential. *International Journal of Coal Geology. 183*, 78-99. DOI: https://doi.org/10.1016/j.coal.2017.09.016

Srivastava, H., Bhaumik, A.K., Tiwari, D., Mohanty, S.P. and Patil, D.J. (2018) Characterization of organic carbon in black shales of the Kachchh basin, Gujarat, India. *Journal of Earth System Science. 127*, 1-12. DOI: https://doi.org/10.1007/s12040-018-1002-8

Wang, X.C., Sun, S., Ma, H.Q. and Liu, Y. (2006) Sources and distribution of aliphatic and polyaromatic hydrocarbons in sediments of Jiaozhou Bay, Qingdao, China. *Marine Pollution Bulletin. 52*(2), 129-138. DOI: https://doi.org/10.1016/j.marpolbul.2005.08.010